

FINAL Rpt.
NGR-49-001-014
Univ. West. Va.

DRF 3594

THERMAL CONTROL CHARACTERISTICS OF
A DIFFUSE BLADED SPECULAR
BASE LOUVER SYSTEM

by

H. W. Butler

J. F. Parmer

E. A. Stipandic

FACILITY FORM 602

N 68-30149

(ACCESSION NUMBER)

(THRU)

58

(PAGES)

(CODE)

CR-95870

(CATEGORY)



ABSTRACT

Movable shutters or louvers systems have been successfully flown on a number of spacecraft missions to ensure temperature control of the spacecraft. Highly polished metallic louver blades mounted over a diffuse white faceplate are now state of the art. However, it was decided to investigate the thermal characteristics of a new configuration incorporating diffuse metallic blades mounted over a specular high solar reflecting base surface.

The investigation includes an analytical determination of all heat transfer characteristics of a louver system operating in full sunlight. This analysis is made with the assumption that definite surface areas of illumination exist on the diffuse blades due to either direct solar impingement or a specular reflection from the base surface. The radiosity approach is used in first writing a solar flux balance and solving for all thermal properties associated with the solar region. A heat balance is then used to determine the terrestrial properties of the system. The solar and terrestrial properties are then superimposed resulting in the determination of the thermal control characteristics of the system.

Results show that unless the spacecraft's stabilization allows the solar polar angle to be held constant at 0° , the louver system cannot operate in full sunlight with a linear actuator mechanism. The new configuration compares favorably with the specular blade diffuse base louver system. Minimum blade temperature average 200°R less for

the diffuse bladed system because of the elimination of multiple specular reflections of the sun's energy by the specular blades. On the average the diffuse bladed system rejects less energy than the specular blade system during the maximum dissipation periods, but it also absorbs less energy during the maximum absorption periods.

Using a modified integrating sphere the solar reflectance of four louver test models was found for various solar polar angles. Experimental results from these tests were found to compare favorably with the analytical results.

NOMENCLATURE

A	albedo irradiance, BTU/hr-ft ²
A _i	area of surface i, ft ²
E _b	emissive power of black body, BTU/hr-ft ²
F(i-j)	view factor from element i to element j, dimensionless
F(i-j) _T	total imaged view factor from element i to element j, dimensionless
G	irradiation of a surface, BTU/hr-ft ²
J	radiosity of a surface, BTU/hr-ft ²
P	planet irradiance, BTU/hr-ft ²
Q _i	internal heat generation, BTU/hr-ft ²
Q _{sbi}	energy absorbed by blade i, BTU/hr-ft ²
Q _{net}	net energy absorbed by base surface, BTU/hr-ft ²
S	solar constant, BTU/hr-ft ²
T	temperature, °R
Y	position on the ordinate, ft
α_i	absorptance of surface i, dimensionless
ϵ_i	emittance of surface i, dimensionless
ρ_i	reflectance of surface i, dimensionless
ρ_{eff_s}	effective solar reflectance of the louver array, dimensionless
σ	Stefan-Boltzman constant, $.1713 \times 10^{-8}$ BTU/hr-ft ² -°R
ϕ	solar polar angle, radians
Θ	louver blade angle, radians

Superscripts

' pertains to second distinct area of illumination on the blade surface

" pertains to third distinct area of illumination on the blade surface

Subscripts

d diffuse

s solar

sp specular

t terrestrial

INTRODUCTION

A revived interest in radiation heat transfer has been stimulated by modern technological advancements, especially in connection with spacecraft missions. For example, in atmosphere-free space, thermal radiation is the major transfer mechanism which allows a spacecraft to reject waste heat.

The temperature of a spacecraft is dependent on the energy absorbed from its environment, the energy emitted from its external surfaces, and its internal heat generation.

The energy absorbed from its environment consists of albedo radiation (energy reflected by a planet or its atmosphere), planet radiation (energy emitted by a planet), and solar radiation (energy emitted by the sun). For steady state equilibrium the temperature of a spacecraft is governed by the equation:

$$A_i \varepsilon_i \sigma T_i^4 = Q_i + A_i F_{(i-s)} \alpha_{si} S + A_i F_{(i-p)} \alpha_p P \quad (1)$$

For an interplanetary spacecraft, or whenever the albedo and planet effects can be neglected, equation 1 reduces to

$$A_i \sigma \varepsilon_i T_i^4 = Q_i + A_i F_{(i-s)} \alpha_{si} S \quad (2)$$

and when solved for temperature

$$T_i = \left[\frac{\frac{Q_i}{A_i} + F_{(i-s)} \alpha_{si} S}{\sigma \varepsilon_i} \right]^{\frac{1}{4}} \quad (3)$$

From equation 3 it is easily seen that an optimal selection of the ratio $\frac{\alpha_s}{\epsilon}$ can be effectively used to obtain spacecraft thermal control if the values of $F_{(i-s)}$, Q_i , and S are constant. However, on an interplanetary mission these quantities are variable. In fact, for example, the solar irradiance, S , at the orbit of Mercury is 6.6 times the solar irradiance at the Earth's orbit. Although S can be considered constant in a planetary mission (Earth orbit), Q_i and $F_{(i-s)}$ vary depending upon the spacecraft's operating power requirements and its orientation respectively. Therefore, due to the variable quantities involved, a system is needed which will allow the ratio $\frac{\alpha_s}{\epsilon}$ to be varied in accordance with the spacecraft's temperature. One method of accomplishing this task is with the use of movable shutters or louvers which are designed to close when the spacecraft temperature drops below a specified limit. The closed louvers then act as a thermal insulator to reduce further heat loss. When heat has to be rejected, the louvers will open, allowing heat to escape.

The louver system consists of movable blades which are mechanically attached to the exterior of the spacecraft. The blades are usually actuated by either bimetallic coils or a bellows system utilizing a vapor-liquid mixture such as Freon II (1). When a bellows system is used a single linkage causes all of the blades to rotate simultaneously.

Presently used louver systems employ highly polished metallic blades which are usually mounted over a diffuse reflecting baseplate. This type of louver system has been used on the Mariner, Nimbus, Pegasus, OSO, and OGO. However, on each spacecraft some type of means has been used to protect the louvers from direct sunlight. With the advent of

larger and more complex spacecraft, a temperature control device may be needed which will function adequately in full sunlight. All previous investigations have been made on specular blade diffuse base louver systems (1-7). With the development of suitable high solar reflecting specular coatings it was decided to investigate the possibility of a new type of louver system satisfactorily operating in direct sunlight. This new louver system consists of metallic diffuse blades mounted on a specular reflecting baseplate. An analysis of all the appropriate thermal control characteristics of this new configuration has been made.

DESCRIPTION OF THE DIFFUSE BLADED SPECULAR BASE LOUVER SYSTEM

This analysis is made for a louver system having blades which are completely diffuse and a base which is specular reflecting and diffuse emitting.

Figure 1 is a sketch of this new louver system illustrating the allowable blade rotation and the sun's positioning. Solar impingement is analyzed for the case when all rays are perpendicular to the axis of rotation of the blades. Since a single actuator may be used to rotate all of the blades, the blade angles are assumed identical. No overlapping of the blades is assumed, therefore, the widths of the blades and base are assumed to be unity.

The blades of the louver system are metallic with a high internal conductance. The blades may be painted to obtain the properties of a high diffuse reflectance and a low terrestrial, i.e. far infrared, emittance. The base of the system has the properties of a high specular reflectance and a high terrestrial emittance. Therefore, the $\frac{\epsilon_s}{\epsilon}$ ratio is very low for the base, thus giving it maximum control over heat dissipation through the array. Since the electronic equipment is located below the base surface, the temperature of the base must be kept within prescribed tolerances. A "super white" surface having the described properties of the base has been developed by Wiebelt (8). It is prepared by evaporating silver on a Vicor micro-cover glass 0.006 inches thick and then overcoating the silver with two coats of aluminum.

The aluminum ensures optical opacity and protects the silver from atmospheric tarnish. This "super white" surface was found to have a solar absorptance of 0.04 and an emittance at 83°F of $0.88 \pm .03$.

ASSUMPTIONS

In order to facilitate the mathematical analysis of the diffuse blades specular base louver system the following assumptions are made:

- 1) The blades form an infinite array so that edge and end effects may be neglected.
- 2) Kirchoff's identity applies in both the solar and infrared wavelength regions so that $\alpha_s = 1 - \rho_s$ and $\rho_t = 1 - \alpha_t = 1 - \epsilon_t$.
- 3) The radiosity of the blades are uniform within defined regions of illumination.
- 4) The internal conductance of the blades and base is infinite so that they are isothermal.
- 5) There is no conduction or convection between surfaces.
- 6) Solar impingement is perpendicular to the axis of rotation of the blades.

The first assumption is reasonable because an array is made up of a large number of blades and the size of one channel is small compared to the size of the entire array. Also a sealed ring is placed around the array facilitating the negligible edge effects assumption. This first assumption allows the thermal events of one channel to be identical to the thermal events of any other channel in the array.

Kirchoff's identity can be proved in an isothermal enclosure (9) and is a reasonable assumption for the case of separate wavelength regions. There are very few materials for which ϵ_λ and α_λ are

constant over the entire range of wavelengths. However, many engineering materials are partially gray; i.e., that is they are gray for some ranges of wavelength. Highly polished aluminum and oxidized aluminum are two of these partially gray materials (10). Since aluminum can be used for both the blades and the base surface the second assumption is valid.

The third assumption was made in order to mathematically analyze the louver system. It is believed to be much better than assuming the entire blades to be of uniform radiosity. The fourth assumption is considered reasonable. Since both the blades and base are metallic, it is reasonable to assume that their internal conductances are large enough to make them essentially isothermal.

The fifth assumption is reasonable since an evaluation of the Nimbus spacecraft shutter system showed heat leakage at the pins and joints to be quite low (1).

The sixth assumption is made in order to make a two dimensional analysis of the louver system.

DETERMINATION OF THERMAL CONTROL CHARACTERISTICS

The incident solar radiation to a diffuse bladed specular base louver system may illuminate a louver section directly, after specular reflection, and after diffuse reflection. Through these methods of illumination four distinct areas may exist on the diffuse blades in the following manner:

- 1) Direct solar impingement plus specular and diffuse reflection
- 2) Direct solar impingement plus diffuse reflection
- 3) Diffuse and specular reflection
- 4) Diffuse reflection only

Illustrations of these distinct areas of illumination are given in Figure 2 in which the numbered areas correspond to the manner in which they are illuminated. Depending upon the blade angle and the solar polar angle a maximum of three and a minimum of one uniformly irradiated area may exist on a single blade.

The irradiation of any of these areas may be calculated by using geometry. For example, consider the irradiation of the louver system in Figure 3 in which three different distinct areas exist on blade 1. These areas are denoted 1, 1', and 1" while their image surfaces are denoted 1,3; 1',3; and 1",3. The points a,b,c,d,f, and g and their images which are denoted by primes are easily located as a function of θ and the Y-intercept of the sun's rays through these points. The

irradiation of area A_1 due only to a specular reflection from surface 3 is;

$$G_{A_1} = \rho_s S |(Y_s - Y_d) \sin \phi| \quad (4)$$

the irradiation of area A_2 due to direct solar impingement is;

$$G_{A_2} = S |(Y_d - Y_f) \sin \phi| \quad (5)$$

the irradiation of surface A_3 due to direct solar impingement is;

$$G_{A_3} = S |(Y_g - Y_d) \sin \phi| \quad (6)$$

The quantity $|(y_i - y_j) \sin \phi|$ represents the projected area normal to the sun.

The total radiosity of a surface, which is the total radiant power leaving the surface per unit area, can be written as

$$J = \rho G_T + \epsilon E_b \quad (7)$$

where:

J is the total radiosity, BTU/hr-sq. ft.

In the solar region E_b is negligible and for the solar radiosity, equation 7 reduces to

$$J = \rho G_T \quad (8)$$

The total irradiation, G_T , is due to direct illumination, specular reflection, and diffuse reflection.

In equations 4, 5, and 6, only the direct illumination and specular reflection were considered. Therefore, considering diffuse reflection,

and with reference to Figure 3: the radiosities of the surface A_1 (a to b) caused by solar radiation is

$$A_1 J_{S1} = \rho_{S1} [G_{A1} + A_1 F_{(1-1)T_s} J_{S1} + A_2 F_{(2-1)T_s} J_{S2} \\ + A_1' F_{(1'-1)T_s} J_{S1'} + A_1'' F_{(1''-1)T_s} J_{S1''}] \quad (9)$$

for surface A_2 (f to g)

$$A_2 J_{S2} = \rho_{S2} [G_{A2} + A_1 F_{(1-2)T_s} J_{S1} + A_2 F_{(2-2)T_s} J_{S2} \\ + A_1' F_{(1'-2)T_s} J_{S1'} + A_1'' F_{(1''-2)T_s} J_{S1''}] \quad (10)$$

for surface A_1' , (b to c)

$$A_1' J_{S1'} = \rho_{S1'} [G_{A1'} + A_1 F_{(1-1')T_s} J_{S1} + A_2 F_{(2-1')T_s} J_{S2} \\ + A_1' F_{(1'-1')T_s} J_{S1'} + A_1'' F_{(1''-1')T_s} J_{S1''}] \quad (11)$$

for surface A_1' , (c to d)

$$A_1' J_{S1'} = \rho_{S1''} [G_{A1''} + A_1 F_{(1-1'')T_s} J_{S1''} + A_2 F_{(2-1'')T_s} J_{S2} \\ + A_1' F_{(1'-1'')T_s} J_{S1''} + A_1'' F_{(1''-1'')T_s} J_{S1''}] \quad (12)$$

Using equations 9, 10, 11, and 12 the four unknown solar radiosities can be determined. Since surface three has been assumed to be specular it has no solar radiosity associated with it (11). A radiosity is associated only with a diffuse surface or the diffuse component of a specular surface. Therefore, there was no reason to consider any distinct areas of illumination on surface three. Once the solar radiosities are known the amount of solar radiation absorbed by each surface area can be determined.

Again assuming that energy emitted in the solar wavelengths is negligible, the solar radiation absorbed by any surface can be written as

$$Q_{si} = \alpha_{si} G_{si} \quad (13)$$

Solving for the irradiation in equation 8 and substituting into equation 13 gives the amount of solar radiation absorbed by any diffuse surface:

$$Q_{si} = \frac{\alpha_{si} J_{si}}{\rho_{si}} \quad (14)$$

For the specular surface A_3 only equation 13 applies for the radiation absorbed,

$$Q_{s3} = \alpha_{s3} [G_{A3} + A_1 F_{(1-3)T_s} J_{s1} + A_2 F_{(2-3)T_s} J_{s3} + A_1' F_{(1'-3)T_s} J_{s1'} + A_1'' F_{(1''-3)T_s} J_{s1''}] \quad (15)$$

Now that all the solar properties of the system have been determined, attention can now be shifted to the terrestrial properties, or those in the infrared region. Using radiant properties characteristic of the two spectral regions (solar and infrared), blade temperature and surface heat-transfer rates can be found by superposition of the solar solution upon the infrared solution. Plamondon (12) showed that this method compares very favorably with the exact method in which radiosity and irradiation are functions of both position and wavelength.

The terrestrial characteristics of the system can be determined by solving the heat balance equations for each surface in the system.

The terrestrial irradiations of blades 1 and 2 can be written:

for blade 1,

$$G_{t_1} = \epsilon_{t_3} \sigma T_3^4 A_3 F_{(3-1)\tau_t} + A_1 F_{(1-1)\tau_t} J_{t_1} + A_2 F_{(2-1)\tau_t} J_{t_2} \quad (16)$$

and for blade 2,

$$G_{t_2} = \epsilon_{t_3} \sigma T_3^4 A_3 F_{(3-2)\tau_t} + A_1 F_{(1-2)\tau_t} J_{t_1} + A_2 F_{(2-2)\tau_t} J_{t_2} \quad (17)$$

Using equation 7 the terrestrial radiosities of the blades can be written:

for blade 1,

$$A_1 J_{t_1} = \rho_{t_1} \left[\sum_{t_3} \sigma T_3^4 A_3 F_{(3-1)T_t} + A_1 F_{(1-1)T_t} J_{t_1} \right. \\ \left. + A_2 F_{(2-1)T_t} J_{t_2} \right] + A_1 \sum_{t_1} \sigma T_1^4 \quad (18)$$

for blade 2,

$$A_2 J_{t_2} = \rho_{t_1} \left[\sum_{t_3} \sigma T_3^4 A_3 F_{(3-2)T_t} + A_1 F_{(1-2)T_t} J_{t_1} \right. \\ \left. + A_2 F_{(2-2)T_t} J_{t_2} \right] + A_2 \sum_{t_2} \sigma T_2^4 \quad (19)$$

Since there is no internal heat generation within the blades, the total energy emitted by them is equal to the total energy absorbed.

Referring to Figure 3 this can be written:

for blade 1,

$$A_1 \sum_{t_1} \sigma T_1^4 = \alpha_{t_1} \left[A_1 F_{(1-1)T_t} J_{t_1} + A_2 F_{(2-1)T_t} J_{t_2} \right. \\ \left. + A_3 \sum_{t_3} \sigma T_3^4 F_{(3-1)T_t} \right] + Q_{SB1} \quad (20)$$

for blade 2,

$$A_2 \sum_{t_2} \sigma T_2^4 = \alpha_{t_2} \left[A_1 F_{(1-2)T_t} J_{t_1} + A_2 F_{(2-2)T_t} J_{t_2} \right. \\ \left. + A_3 \sum_{t_3} \sigma T_3^4 F_{(3-2)T_t} \right] + Q_{SB2} \quad (21)$$

where

Q_{SBI} is the total solar energy absorbed by blade 1, BTU/hr-ft²

or

$$Q_{SBI} = Q_{SI} + Q_{SI'} + Q_{SI''} \quad (22)$$

Since the blades are assumed isothermal $T_1 = T_2$ and the blades are of equal area $A_1 = A_2$, equations 20 and 21 can be reduced to,

$$A_1 \sigma T_1^4 (\varepsilon_{t_1} + \varepsilon_{t_2}) = \alpha_{t_1} [A_1 F_{(1-1)T_e} J_{t_1} + A_2 F_{(2-1)T_e} J_{t_2}]$$

$$+ A_3 \varepsilon_{t_3} \sigma T_3^4 F_{(3-1)T_e} \left] + \alpha_{t_2} [A_1 F_{(1-2)T_e} J_{t_1} + A_2 F_{(2-2)T_e} J_{t_2}] \right]$$

$$+ A_3 \varepsilon_{t_3} \sigma T_3^4 F_{(3-2)T_e} \left] + Q_{SBI} + Q_{SB2} \quad (23) \right.$$

Equations 18, 19, and 22 can now be solved for T_1 , J_{t_1} , and J_{t_2} .

The amount of emitted energy absorbed by each surface may then be calculated by the following relations:

$$Q_{t_1} = \frac{\alpha_{t_1}}{\rho_{t_1}} (J_{t_1} - E_{t_1}) \quad (24)$$

$$Q_{t_2} = \frac{\alpha_{t_2}}{\rho_{t_2}} (J_{t_2} - E_{t_2}) \quad (25)$$

where

$$Q_{t_3} = \alpha_{t_3} [A_1 F_{(1-3)T_e} J_{t_1} + A_2 F_{(2-3)T_e} J_{t_2}] \quad (26)$$

Q_{t_i} is the amount of terrestrial energy absorbed by surface i , BTU/hr-ft²

E_{t_i} is the emissive power of surface i , BTU/hr-ft²

The net energy transfer at the base is the difference between the emissive power and the total energy absorbed,

$$Q_{NET3} = \epsilon_{t3} A_3 \sigma T_3^4 - (Q_{S3} + Q_{t3}) \quad (27)$$

The sign convention adopted is that a positive Q_{net} means heat is being rejected.

CALCULATION OF EFFECTIVE SOLAR REFLECTANCE

In Figure 3 it is seen that the amount of energy escaping from the channel is a function of both the blade angle and the solar polar angle. The effective solar reflectance may be defined as the ratio of the solar energy out to the solar energy into the channel. Considering area A_4 to be space at $0^\circ R$ the solar energy out of the channel is (Figure 3)

$$Q_{out_s} = A_1 F_{(1-4)T_s} J_{s1} + A_2 F_{(2-4)T_s} J_{s2}$$

$$+ A_1' F_{(1'-4)T_s} J_{s1'} + A_1'' F_{(1''-4)T_s} J_{s1''} \quad (28)$$

and

$$Q_{in} = S \cos \phi \quad (29)$$

Therefore the effective solar reflectance

$$\rho_{eff_s} = \frac{Q_{out}}{Q_{in}} \quad (30a)$$

$$\rho_{\text{eff},s} = \frac{A_1 F_{(1-4)T_s} J_{S1} + A_2 F_{(2-4)T_s} J_{S2} + A_1' F_{(1'-4)T_s} J_{S1'} + A_1'' F_{(1''-4)T_s} J_{S1''}}{S \cos \phi} \quad (30b)$$

The effective solar reflectance may also be experimentally determined in an integrating sphere and the results compared to the analytical results.

CALCULATION OF TOTAL IMAGED VIEW FACTORS

Although a number of methods for determining view factors are available, Hottel's crossed string method (13) lends itself to the situation of louver systems, especially when blockage is involved. In this method flux algebra and the assumption that the areas involved are infinite in length (in the direction normal to the plane of the paper in Figure 4) are used to show that,

$$A_1 F_{(1-2)} = \frac{(\text{sum of crossed strings}) - (\text{sum of uncrossed strings})}{2} \quad (31)$$

Referring to Figure 9, the string distances are the dotted lines or,

$$A_1 F_{(1-2)} = \frac{\overline{ad} + \overline{bc} - (\overline{ac} + \overline{bd})}{2} \quad (32)$$

where

\overline{ad} is the length of the imaginary tightly stretched string between the points a and d

It should be noted that the stretched string must pass through a specular surface in determining the view factor between an image surface and any other surface, but the string cannot pass through a diffuse surface. This restriction can be further explained by considering the louver system arrangement in Figure 3. Since an observer located anywhere on the image surface 1", 3 cannot "see" surface 2,

$$F_{(1'', 3-2)} = 0$$

An observer on the image surface 1,3 can "see" surface 2 from any point on surface 1,3. Therefore, the view factor from 1,3 to 2 is

$$F_{(1,3-2)} = \frac{\overline{ad} + \overline{b'f} - (\overline{af} + \overline{b'd})}{2 \overline{ab'}} \quad (33)$$

However, an observer on the image surface 1',3 cannot always "see" surface 2. Remembering that the stretched string cannot pass through a diffuse surface the view factor from the surface 1',3 to surface 2 is

$$F_{(1',3-2)} = \frac{\overline{b'd} + \overline{df} - (\overline{b'f} + \overline{c'd}) + \overline{c'd}}{2 \overline{b'c'}} \quad (34)$$

Using a fixed coordinate system and a logic system involving Y intercepts of various points on the louver system, a digital computer program was devised to calculate the necessary total imaged view factors as a function of both the blade angle and the solar angle. The digital computer program appears in Appendix A.

RESULTS

Because of the complexity of the equations governing the thermal control characteristics of the louver system it was necessary to use the IBM 7040 computer in order to obtain numerical solutions. Solutions were obtained for θ from 0° to 90° and for ϕ from -90° to 90° , both in any desired increment. The results given in Figures 5a, b, c, d are for a louver system having blade properties $\rho_s = 0.80$ and $\epsilon_t = 0.10$, base properties $\rho_b = 0.90$ and $\epsilon_b = 0.85$, and a base temperature of $530^\circ R$. The chosen base temperature is typical of spacecraft requirements. The chosen blade and base properties are representative of a combination which is easily obtainable. In Figures 5a-d the amount of heat absorbed by the base is divided into two components. The curve associated with the hatched area represents the solar energy absorbed by the base. The middle curve represents the terrestrial energy absorbed by the base. This is due to the temperature of the blades and the temperature of the base itself. The top curve represents the total amount of energy absorbed by the base surface.

Notice in each of the figures that the maximum amount of solar energy absorbed occurs whenever $\theta + \phi = 90^\circ$. At this position the blades receive no direct solar impingement; thus the base area is entirely irradiated. However, this particular combination of θ and ϕ does not always result in the worst heat rejection case. For instance when $\phi = 0$ (Figure 5a), the maximum solar energy absorbed occurs

when $\Theta + \Phi = 90$, but this is also the position for the minimum amount of the total and terrestrial energy being absorbed. Therefore, in this case the terrestrial energy is the dominate factor and maximum heat dissipation occurs whenever it is a minimum. It also should be noted that if the spacecraft could be positioned such that $\Phi = 0^\circ$ at all times, then a linear actuator louver mechanism could be used in full sunlight with a maximum heat dissipation of 40.6 BTU/hr-ft^2 . This is of course neglecting albedo, solar panel input, and any other heat inputs to the louver system.

In Figures 5.c, d it is seen that the worst heat rejection does occur when $\Theta + \Phi = 90^\circ$. However, in Figure 5.b ($\Phi = 20$) the worst case occurs when the louvers are fully closed, but the maximum heat rejection is accomplished when $\Theta - \Phi = 90^\circ$. Figures 5a-d indicate that unless Φ is held at 0° then a linear actuated louver system will not function properly in sunlight.

In Figures 6.a, 7a the thermal characteristics of the particular system investigated are given for various solar polar angles. Notice that the blade temperature increases for $\Phi = 0^\circ$ to $\Phi = 30^\circ$ while the heat rejection capacity decreases in the same limit. However, due to the geometry of the system, the heat rejection capacity increases as Φ increases from 30° while the blade temperatures decrease in the same limit.

Figures 6.b, c, 7b, c show the thermal characteristics of louver systems with various other properties. Notice that by changing the properties, the maximum and minimum heat dissipation may be influenced. For instance in Figure 7.c the differences between the heat rejections

for the fully closed and fully opened positions are much less than the corresponding differences in Figure 7a. It would seem that maximum thermal control would be achieved when these differences reached a maximum. However, mission requirements may dictate a system with thermal characteristics similar to those in Figure 7c.

In Figures 8a, b, c, d the results of the experimental determination of solar reflectance are compared to the analytical results. Notice that the trend of the experimental results to run higher or lower than the analytical results is not the same for both negative and positive values of ϕ . This can be explained very simply since the test sample had to be reoriented and the optics system altered when proceeding from a positive to a negative and resulting in a loss of similarity.

The scattering of radiation in the plane of the blades due to their diffuse property was found to be a significant factor of error. The inability of attaining a perfectly parallel beam of incident radiation also resulted in an increase in the scattering. Some difficulty is evidenced in the correlation of the analytical and experimental results because the experiment involved a finite sample size and a finite width of impinging radiation, both of which contradict the assumptions of the analytical solution.

CONCLUSIONS

Initially it was thought that with the development of new specular reflecting coatings with very low $\frac{\epsilon_s}{\epsilon}$ ratios, an improved louver system could be designed utilizing a specular base and diffuse blades. The advantage of the low $\frac{\epsilon_s}{\epsilon}$ specular base is that it allows the system to attain a high effective solar reflectance. The reduction in the trapping effect of the sun's energy caused by multiple reflections, the attainment of considerably lower blade temperatures, and the low solar absorptance of solar energy appear to be the main advantages of the new configuration over the specular blade diffuse base louver system. However, this analysis shows that this system will not perform satisfactorily in sunlight with a linear actuator. This is the same problem encountered with the specular blade louver system. Since heat rejection for the louver system is a function of both blade angle and solar polar angle, a nonlinear actuator could not be used. A logical control system could be devised, but it would be questionable whether the effectiveness could outweigh the cost. Shielding of the louvers has been studied, but the maximum dissipation is considerably decreased whenever a thermal barrier is used.

Further investigations into improvements of louver system may be along the lines of a completely specular system with the base and the underside of the blades coated with a low $\frac{\epsilon_s}{\epsilon}$ material.

BIBLIOGRAPHY

1. London, A. "Shutter System Design for Nimbus Spacecraft." A.I.A.A. Paper 67-309.
2. Plamondon, J. A. "Analysis of Movable Louvers for Temperature Control". Journal of Spacecraft and Rockets, Vol. 1, No. 5, September-October, 1964.
3. Ollendorf, S. "Analytical Determination of the Effective Emittance of an Insulated Louver System". A.I.A.A. Paper 65-425.
4. Clausen, O. W. and Neu, J. T. "The Use of Directionally Dependent Radiation Properties for Spacecraft Thermal Control". Astronautica Acta, Vol. II, No. 5, 1965.
5. Russell, L. and Linton, R. "Experimental Studies of Pegasus Thermal Control Louver System". A.I.A.A. Paper 67-308.
6. Parmer, J. F. and Buskirk, D. L. "The Thermal Radiation Characteristics of Spacecraft Temperature Control Louvers in the Solar Space Environment". A.I.A.A. Paper 67-307.
7. Parmer, J. F. and Buskirk, D. L. "Thermal Control Characteristics of Interior Louver Panels". A.S.M.E. Paper 67-HT-64.
8. Wiebelt, J. A. "Progress Report on NASA NsG-454". December 1966.
9. Wiebelt, J. A. Engineering Radiation Heat Transfer, New York, New York, Holt, Rinehart, Winston, 1966.
10. Singham, J. R. "Tables of Emissivities of Surfaces". International Journal of Heat and Mass Transfer, U. S., 1962, pp. 67-76.
11. Holman, J. P. "Radiation Networks for Specular-Diffuse Reflecting and Transmitting Surfaces". A.S.M.E. Paper 66 WA/HT-9.
12. Plamondon, J. A. and Landram, C. S. "Radiant Heat Transfer from Nongray Surfaces with External Radiation". A.I.A.A. Paper 66-21.
13. McAdams, W. H. Heat Transmission, New York, New York, McGraw Hill, 1954, Chapter 4 by Nottel.

APPENDIX A

COMPUTER PROGRAM DESCRIPTION

A digital computer program has been written for the analysis of a diffuse bladed specular base louver system in which the blade angle may assume any value from 0° to 90° and the solar polar angle may take on any value from -90° to 90° .

In the digital computer program all louver characteristics in the solar region of the spectrum are determined first for a positive and then for a negative solar polar angle. After all solar characteristics are found, the terrestrial characteristics are determined. No subroutines are used except for LNEQNS, which is a Watfor subroutine for a solution of N simultaneous equations.

In order to decrease computer time, no louver properties were subscripted. Therefore, all properties desired must be printed out simultaneously for each particular blade angle and solar polar angle encountered.

NOMENCLATURE

A1, A1P, A1PP, A2	areas of surfaces 1, 1', 1'', and 2 respectively, ft^2
BB1, BB2, BB3, BB4	solar radiosities of surfaces 1, 2, 1', and 1'' respectively, $\text{BTU}/\text{hr}\cdot\text{ft}^2$

F1P2	area of surface 1 times the diffuse view factor from surface 1 to 2, dimensionless
F1P2T	area of surface 1 times the total imaged view factor from surface 1 to 2, dimensionless
G1, G2, G1P, G1PP	irradiation of surfaces 1, 2, 1', and 1" due to direct impingement of a specular reflection, BTU/hr-ft ²
PH1	solar polar angle, degrees
RAD1, RAD2	terrestrial radiosities of blades 1 and 2 respectively, BTU/hr-ft ²
THETA	blade angle, degrees
W1, W2, W4	projected area of direct illumina- tion of blade 1, the base, and blade 2 respectively, BTU/hr-ft ²
W31, W32	projected area of specularly re- flected illumination of blades 1 and 2 respectively, BTU/hr-ft ²
X1P, Y1P, X2P, Y2P	coordinates of points of inter- section of surfaces 1 and 1', 1' and 1" respectively, ft
Yi	Y-intercept of a ray passing through point i, ft

INPUT DATA

The program input data is listed on five cards with format field of 10 spaces for each quantity on each card.

Card 1.	XNT	XNP		
Card 2.	RH01	RH02	RH03	P
Card 3.	THEMIN	THEMAX	PHIMIN	PHIMAX
Card 4.	ALPHA1	ALPHA2	ALPHA3	
Card 5.	EMM1	EMM2	EMM3	T3

where:

XNT - size of blade angle increment, degrees

XNP - size of solar polar angle increment, degrees

RH01, RH02, RH03 - solar reflectance of surfaces 1, 2, and 3
respectively, dimensionless

P - solar radiation intensity, BTU/hr-ft²

THEMIN - minimum blade angle ($\angle 0^\circ$), degrees

THEMAX - maximum blade angle ($\angle 90^\circ$), degrees

PHIMIN - minimum solar polar angle ($\angle -90^\circ$), degrees

PHIMAX - maximum solar polar angle ($\angle 90^\circ$), degrees

ALPHA1, ALPHA2, ALPHA3 - solar absorptance of surfaces 1, 2, and
3 respectively, dimensionless

EMM1, EMM2, EMM3 - terrestrial emittance of surfaces 1, 2, and 3
respectively, dimensionless

T3 - temperature of base surface, °R

PRINTED OUTPUT

As the program is now listed the printed output contains first an echo check of all data input and the following:

QABS1, QABS2, QABS3 - solar energy absorbed by surfaces 1, 2, and 3 respectively, BTU/hr-ft²

REFLEC - effective solar reflectance, dimensionless

Q1, Q2, RQABS3 - energy absorbed by surfaces 1, 2, and 3 respectively in the infrared region, BTU/hr-ft²

QNET - net thermal energy absorbed by base surface (assumed positive when rejecting heat), BTU/hr-ft²

C W2 IS WHAT STRIKES THE BASE
 C W4 IS WHAT STRIKES BLADE 2 DIRECTLY
 C W31 IS WHAT IS REFLECTED TO BLADE 1
 C W32 IS WHAT IS REFLECTED TO BLADE 2
 C XNT IS THE INCREMENT ON THETA
 C XNP IS THE INCREMENT ON PHI
 C FXYT IS THE TOTAL VIEW FACTOR FROM X TO Y
 C RHO1 IS THE SOLAR REFLECTANCE OF BLADE 1
 C RHO2 IS THE SOLAR REFLECTANCE OF BLADE 2
 C RHO3 IS THE SOLAR REFLECTANCE OF THE BASE
 C NOTE ALL VIEW FACTORS ARE ACTUALLY AX*(FXY)
 DIMENSION A(4,4),B(4)
 READ(5,99) XNT,XNP
 99 FORMAT(F10.1,F10.1)
 READ(5,91) RHO1,RHO2,RHO3,P
 91 FORMAT(4(F10.2))
 READ(5,220) THEMIN,THEMAX,PHIMIN,PHIMAX
 220 FORMAT(4(F10.3))
 READ(5,54) ALPHA1,ALPHA2,ALPHA3
 54 FORMAT(3(F10.3))
 READ(5,44) EMM1,EMM2,EMM3,T3
 44 FORMAT(4(F10.3))
 KS=THEMIN+1.
 KE=THEMAX+1.
 JE=91.+PHIMAX
 JS=91.+PHIMIN
 SIGMA=.1714E-08
 NT=XNT
 NP=XNP
 K=0
 KK=0
 CONV=3.1415926/180.
 WRITE(6,50) RHO1,RHO2,RHO3,ALPHA1,ALPHA2,/ALPHA3
 50 FORMAT(4X,12HECHO CHECK,///,15X,5HSOLAR,/,10X,5HRHO1=F8.3,/,10X,
 1X,5HRHO2=F8.3,/,10X,5HRHO3=F8.3,/,10X,7HALPHA1=F8.3,/,10X,7HALPHA2=
 2F8.3,/,10X,7HALPHA3=F8.3,/,10X,7HALPHA3=,F8.3,///)
 WRITE(6,238) EMM1,EMM2,EMM3,T3
 238 FORMAT(15X,11HTERRESTRIAL,/,10X,12HEMMISIVITY1=F8.3,/,10X,
 112HEMMISIVITY2=F8.3,/,10X,12HEMMISIVITY3=F8.3,/,10X,10HBASE TEMP=
 2F10.3,///)
 WRITE(6,57)
 57 FORMAT(26X,5HTHETA,24X,11HTERRESTRIAL,//)
 WRITE(6,61)
 61 FORMAT(1X,5HTHETA,3Y,3Hphi,4X,5HQABS1,3Y,5HQABS2,3X,5HQABS3,3Y,
 16HREFLEC,2X,5HQABS1,3X,5HQABS2,3X,5HQABS3,3X,4HRAD1,4X,4HRAD2,3X,
 27HBL TEMP,3X,4HQNET)
 DO 10 J=KS,KE,NT
 THETA=J-1
 ZT=CONV*THETA
 R=COS(ZT)
 S=SIN(ZT)
 A11=1.+R
 B11=1.+S
 AS=1.-R
 K=K+1
 DO 10 I=JS,JE,NP
 KK=KK+1

```

PHI=I-91
ZP=CONV*PHI
ZPA=ARS(ZP)
ZPA90=(CONV*90.)-ZPA
IF(PHI.LE.0.) GO TO 5
Z90=(CONV*90.)-ZP
Y1=SIN(ZT)+TAN(Z90)*COS(ZT)
Y2=0.0
Y3=SIN(ZT)+TAN(Z90)*(1.+COS(ZT))
Y4=TAN(Z90)
Y5=-SIN(ZT)+TAN(Z90)*(1.+COS(ZT))
W1=0.0
IF(Y1.EQ.Y3) W4=0.0
IF(Y1.LE.Y4) W4=(Y3-Y4)*(SIN(ZP))
IF(Y1.GT.Y4) W4=(Y3-Y1)*(SIN(ZP))
IF(Y1.GE.Y4) W2=0.0
IF(Y1.LT.Y4) W2=(Y4-Y1)*(SIN(ZP))
IF(Y1.GE.Y4) W32=0.0
IF(THETA.LE.60.) GO TO 20
IF((Y4.GE.Y5).AND.(Y5.GE.Y1)) W32=(Y4-Y5)*(SIN(ZP))
IF((Y1.GE.Y5).AND.(Y4.GE.Y1)) W32=(Y4-Y1)*(SIN(ZP))
GO TO 22
20 W32=0.0
W31=0.0
22 CONTINUE
GO TO 30
C NOW FOR PHI = 0 OR NEGATIVE
5 Y1=SIN(ZT)-(TAN(ZPA90))*(COS(ZT))
Y2=0.0
Y3=SIN(ZT)-(TAN(ZPA90))*(1.+COS(ZT))
Y4=-TAN(ZPA90)
Y5=-(SIN(ZT)+(TAN(ZPA90))*(COS(ZT)))
IF(PHI.EQ.0.0) GO TO 29
W32=0.0
AP=ABS(PHI)
ZO=THETA+AP
IF(ZO.EQ.90.) GO TO 200
IF(Y3.GE.Y2) W2=0.0
IF((Y1.GE.Y2).AND.(Y2.GE.Y3)) W2=(Y2-Y3)*(SIN(ZPA))
IF((Y1.LE.Y2).AND.(Y4.GE.Y3)) W2=(Y1-Y4)*(SIN(ZPA))
IF(Y1.EQ.Y3) W1=0.0
IF((Y1.GT.Y2).AND.(Y3.GE.Y2)) W1=(Y1-Y3)*(SIN(ZPA))
IF((Y1.GT.Y2).AND.(Y2.GT.Y3)) W1=(Y1-Y2)*(SIN(ZPA))
IF(Y1.GT.Y2) W4=0.0
IF(Y2.GE.Y1) W4=(Y4-Y3)*(SIN(ZPA))
IF(Y2.GE.Y1) W1=0.0
IF(Y3.GE.Y2) W31=0.0
IF((Y2.GE.Y3).AND.(Y1.GE.Y2).AND.(Y3.GE.Y5)) W31=(Y2-Y3)*SIN(ZPA)
IF((Y2.GE.Y3).AND.(Y1.GE.Y2).AND.(Y3.LT.Y5)) W31=(Y2-Y5)*SIN(ZPA)
IF((Y2.GT.Y3).AND.(Y2.GT.Y1)) GO TO 100
GO TO 101
100 IF(Y4.GT.Y5) W31=(Y1-Y4)*(SIN(ZPA))
IF(Y4.LE.Y5) W31=(Y1-Y5)*(SIN(ZPA))
101 CONTINUE
GO TO 30
29 W32=0.0
W31=0.0

```

```

W1=0.0
W2=1.0-COS(ZT)
W4=COS(ZT)
30  CONTINUE
    GO TO 201
200  W1=0.0
    W4=0.0
    IF(Y4.GT.Y5) W31=(Y1-Y4)*(SIN(ZPA))
    IF(Y4.LE.Y5) W31=(Y1-Y5)*(SIN(ZPA))
    W32=0.0
    W2=(Y2-Y4)*(SIN(ZPA))
201  CONTINUE
    IF(PHI.LE.0.0) W5=W2-W31
    IF(PHI.GT.0.0) W5=W2-W32
    SUMW=W1+W2+W4
    CP=COS(ZPA)
    ZA=((180.-THETA)/2.)*CONV
    ZB=(THETA/2.)*CONV
    ZZP=SQRT((1.-R)**2+S**2)
    ZUP=SQRT((1.+R)**2+S**2)
    HD=2.*S
    DH=HD
    HE=SQRT(1.+HD**2)
    HJ=SQRT((1.-R)**2+S**2)
    AE=SQRT(A11**2+S**2)
    DJ=2.*SIN(ZB)
C     SPECIAL CASE NEEDED WHEN THETA=90
    IF(THETA.NE.90.) GO TO 509
    X1P=0.
    IF(PHI.GE.0.) W31=W32
    IF(ABS(PHI).EQ.45.) GO TO 412
    IF(W31.GT..00001) GO TO 411
    IF(PHI.EQ.0.) GO TO 412
    Y1P=1.-TAN(ZPA90)
    GO TO 413
412  Y1P=1.
    GO TO 413
411  Y1P=TAN(ZPA90)-1.
    IF(Y1P.GT.1.) Y1P=1.
413  X2P=1.+X1P
    Y2P=Y1P
    IF(PHI.GT.0.) W1=W4
    A1=1.
    A2=Y1P
    A2P=1.-A2
    WP=A2P*SIN(ZPA)
    G2=(W31*RHO3+(W1-WP))*P
    G2P=W2*P
    MA=3
    IF(Y1P.EQ.1.) MA=2
    GO TO 53
509  IF(PHI.LE.0.0) GO TO 508
C     FOR PHI POSITIVE
    MA=3
    PU=THETA+PHI
    YDIF=ABS(Y1-Y4)
    IF(YDIF.LE..00001) GO TO 935

```

IF((PU.EQ.90.) .AND. (THETA.GE.60.) .AND. (W32.NE.0.)) GO TO 935
 IF(Y5.GE.Y1) GO TO 934
 IF(W32.EQ.0.0) GO TO 934
 X2P=(TAN(ZT)-Y1)/(TAN(ZT)-TAN(ZPA90))
 Y2P=(TAN(ZT))*X2P-TAN(ZT)
 Y15=Y2P+(TAN(ZPA90))*X2P
 IF(Y3.GT.Y15) W2P=(Y3-Y15)*SIN(ZP)
 IF(Y3.LE.Y15) W2P=0.0
 GO TO 988
 934 IF(Y1.GT.Y4) GO TO 928
 935 MA=2
 X2P=1.0/R
 Y2P=S
 W2P=0.0
 GO TO 988
 928 X2P=(TAN(ZT)+Y1)/(TAN(ZT)+TAN(ZPA90))
 Y2P=-TAN(ZPA90)*X2P+Y1
 Y15=Y2P+(TAN(ZPA90))*X2P
 W2P=(Y3-Y15)*SIN(ZP)
 988 A1=1.
 A2=(X2P-1.0)/R
 A2P=1.0-A2
 G2=(RH03*W32+(W4-W2P))*P
 G2P=W2P*P
 53 CONTINUE
 ZB=(THETA/2.0)*CONV
 ZEP=SQRT(X2P**2+Y2P**2)
 ZYP=SQRT((S-Y2P)**2+(X2P-R)**2)
 ZSP=SQRT((S+Y2P)**2+(X2P-R)**2)
 F12=(2.*SIN(ZB)+ZEP-(1.0+ZYP))/2.
 IF(THETA.GE.60.) GO TO 923
 F132P=(A2P+ZEP-ZUP)/2.
 F132=(1.0+A2-ZEP)/2.
 GO TO 924
 923 F132=(1.0+ZSP-(ZEP+ZZP))/2.
 F132P=(SQRT(1.0+(2.*S)**2)+ZEP-(ZUP+ZSP))/2.
 924 F12T=F12+RH03*F132
 F12P=(ZUP+ZYP-(1.0+ZEP))/2.
 F12PT=F12P+RH03*F132P
 F11T=RH03*(1.0-S)
 F24=(1.0+ZYP-ZZP-A2P)/2.
 F2P4=(1.0+A2P-ZEP)/2.
 F14=1.0-SIN(ZA)
 IF(THETA.LE.60.) GO TO 26
 F134=(2.*S+2.*SIN(ZA)-1.0-SQRT(1.0+(2.*S)**2))/2.
 F234=(ZZP+A2-ZSP)/2.
 F2P34=(ZZP+1.0-SQRT(1.0+(2.*S)**2)-A2)/2.
 GO TO 27
 26 F234=C.
 F2P34=0.
 F134=(2.*S+2.*SIN(ZA)-2.0-SQRT((1.0-R)**2+S**2))/2.
 27 F24T=F24+RH03*F234
 F2P4T=F2P4+RH03*F2P34
 F14T=F14+RH03*F134
 TOTF12=F12T+F12PT
 400 A(1,1)=RH01*F11T-A1
 A(1,2)=RH01*F12T

```

A(1,3)=RHO1*F12PT
A(2,1)=RHO2*F12T
A(2,2)=-A2
A(2,3)=0.0
A(3,1)=RHO2*F12PT
A(3,2)=0.0
A(3,3)=-A2P
B(1)=0.0
B(2)=-RHO2*G2
B(3)=-RHO2*G2P
CALL LNEQNS (A,MA,B)
ENRGIN=P*COS(ZPA)
IF(MA.EQ.2)B(3)=0.
ENGOUT=RHO3*W5*P+B(1)*F14T+B(2)*F24T+B(3)*F2P4T
REFLEC=ENGOUT/ENRGIN
BB1=B(1)
BB2=B(2)
IF(PHI.GT.0.)GO TO 240
C ONLY FOR PHI NEGATIVE AND THETA=90.
B(1)=BB2
B(2)=BB1
B(4)=0.
A1=Y1P
A1P=1.-Y1P
A1PP=0.
A2=1.
240 CONTINUE
GO TO 65
C FOR PHI NEGATIVE AND = 0
508 PU=THETA+ABS(PHI)
IF((PU.EQ.90.)*AND.(THETA.LT.60.))GO TO 503
IF((Y1.GE.Y2).*AND.(Y2.GT.Y3).*AND.(Y5.GE.Y3)) GO TO 403
IF ((Y2.GE.Y1).*AND.(Y4.LE.Y5).*AND.(Y2.GT.Y3)) GO TO 501
IF ((Y2.GE.Y1).*AND.(Y4.GE.Y5).*AND.(Y2.GT.Y3)) GO TO 506
IF((Y1.GE.Y2).*AND.(Y2.GT.Y3).*AND.(Y5.LE.Y3)) GO TO 503
IF (Y3.GT.Y2) GO TO 504
GO TO 10
C FIGURE 5
403 X1P=R
Y1P=S
X2P=R
Y2P=S
G1=(W1+RHO3*W31)*P
G1P=0.0
G1PP=0.0
GO TO 502
C FIGURE 2
501 X1P=-Y1/(TAN(ZT)+TAN(ZPA90))
Y1P=(TAN(ZT))*X1P
G1=0.
G1P=RHO3*W31*P
G1PP=0.
X2P=R
Y2P=S
GO TO 502
C FIGURE 1
506 G1=0.

```

G1P=RHO3*W31*X_P
 G1PP=0.
 X2P=-Y4/(TAN(ZT)+TAN(ZPA90))
 Y2P=(TAN(ZT))*X2P
 X1P=-Y1/(TAN(ZT)+TAN(ZPA90))
 Y1P=(TAN(ZT))*X1P
 GO TO 516

C FIGURE 3
 503 X1P=((TAN(ZPA90))*A11)-SIN(ZT)/(TAN(ZT)+TAN(ZPA90))
 Y1P=(TAN(ZT))*X1P
 X2P=R
 Y2P=S
 Y7=Y1P-(TAN(ZPA90))*X1P
 W1P=(Y1-Y7)*(SIN(ZPA))
 W13=W1-W1P
 G1=(W13+RHO3*W31)*P
 G1P=W1P*P
 G1PP=0.
 GO TO 502

C FIGURE 4
 504 X1P=(S-(TAN(ZPA90))*A11)/(TAN(ZT)-TAN(ZPA90))
 Y1P=(TAN(ZT))*X1P
 X2P=R
 Y2P=S
 G1=C.
 G1P=W1*P
 G1PP=0.
 502 CONTINUE
 MA=3
 GO TO 515

516 MA=4
 515 CONTINUE
 Y1C=-TAN(ZT)
 Y9=-(Y2P/(1.-X2P))*X2P-Y2P
 Y19=-Y1P-(Y1P/(1.-X1P))*X1P
 A1=X1P/R
 A1P=(X2P/R)-A1
 A1PP=1.-A1-A1P
 A2=1.
 C REFER TO FIGURE FOR EXPLANATION OF TERMS
 DE=1.
 AD=1.
 AJ=1.
 EJ=1.
 BE=SQRT((A11-X1P)**2+(S-Y1P)**2)
 AB=X1P/R
 AC=X2P/R
 CD=1.-AB
 CO=1.-AC
 FD=SQRT((R-X1P)**2+(S+Y1P)**2)
 FE=SQRT((A11-Y1P)**2+(S+Y1P)**2)
 CE=SQRT((A11-X2P)**2+(S-Y2P)**2)
 GE=SQRT((A11-X2P)**2+(S+Y2P)**2)
 GD=SQRT((R-X2P)**2+(S+Y2P)**2)
 BJ=SQRT((1.-X1P)**2+Y1P**2)
 CJ=SQRT((1.-X2P)**2+Y2P**2)
 FJ=FJ

GJ=CJ
 DJ=HJ
 $CF = \text{SQRT}((X2P-X1P)^{*2} + (Y2P-Y1P)^{*2})$
 $CH = \text{SQRT}((R-X2P)^{*2} + (S+Y2P)^{*2})$
 BF=2.*Y1P
 CG=2.*Y2P
 $BH = \text{SQRT}((R-X1P)^{*2} + (S+Y1P)^{*2})$
 BG=CF
 DG=CH
 AF=AB
 C NOTE THESE FIRST 6 VIEW FACTORS ARE NOT MULTIPLIED BY RHC3
 $F1PP31 = (BG+AD-(AC+BH))/2.$
 $F131P = (BF+AC-(CF+AB))/2.$
 $F1PP1P = (BH+CG-(BG+CH))/2.$
 C $F1DP=F1PP31PP$
 $F1DP=(CH+DG-(DH+CG))/2.$
 $F1P31P=(BG+CF-(PF+CG))/2.$
 $F131=(AF+AR-BF)/2.$
 $F14=(BE+AD-(AE+BD))/2.$
 $F12=(AE+BJ-(BE+AJ))/2.$
 $F1P4=(BD+CE-(BE+CD))/2.$
 $F1P2=(BE+CJ-(BJ+CE))/2.$
 $F1PP4=(CD+DE-CE)/2.$
 $F1PP2=(DJ+CE-(DE+CJ))/2.$
 $F134=(FD+AE-(FE+AD))/2.$
 $F1P34=(GD+FE-(GE+FD))/2.$
 $F1PP34=(HD+GE-(HE+GD))/2.$
 $F132=(AJ+FE-(AE+FJ))/2.$
 $F1P32=(GE+FJ-(GJ+FE))/2.$
 $F1PP32=(HE+GJ-(HJ+GE))/2.$
 $F24=(2.-DJ)/2.$
 IF (THETA.GT.60.) F234=(2.*((1.+SIN(7E))-(1.+SQRT(1.+(2.*E)**2))))/2.
 IF (THETA.LT.-60.) F234=0.
 IF (THETA.GE.60.) GO TO 174
 $F1PP34=(HD+GJ+EJ-(GD+EJ+HJ))/2.$
 IF (Y10.GE.Y19) GO TO 175
 IF ((Y10.LT.Y19).AND.(Y10.GE.Y9)) GO TO 177
 IF (Y10.LT.Y9) GO TO 178
 GO TO 10
 175 $F1P32=0.$
 $F1PP32=0.$
 $F1P34=(GD+FJ+EJ-(FD+GJ+EJ))/2.$
 $F134=(FD+AE-(AD+FJ+FJ))/2.$
 $F132=(AJ+FJ+EJ-(AE+FJ))/2.$
 GO TO 174
 177 $F1P34=(GD+FE-(FD+GJ+EJ))/2.$
 $F1P32=(FJ+GJ+EJ-(FE+GJ))/2.$
 $F1PP32=0.$
 GO TO 174
 178 $F1PP32=(GJ+HJ+EJ-(GE+HJ))/2.$
 $F1PP34=(HD+GE-(GD+FJ+HJ))/2.$
 174 CONTINUE
 $F12T=F132*RHO3+F12$
 $F1P2T=F1P2+RHO3*F1P32$
 $F1PP2T=F1PP2+RHO3*F1PP32$
 $F14T=F14+RHO3*F134$
 $F1P4T=F1P4+RHO3*F1P34$

$F1PP4T = F1PP4 + RH03 * F1PP34$
 $F24T = F24 + RH03 * F234$
 $TOTF12 = F12T + F1P2T + F1PP2T$
 $A(1,1) = RH01 * RH03 * F131 - A1$
 $A(1,2) = RH01 * F12T$
 $A(1,3) = RH01 * RH03 * F131P$
 $A(1,4) = RH01 * RH03 * F1PP31$
 $A(2,1) = RH02 * F12T$
 $A(2,2) = -A2$
 $A(2,3) = RH02 * F1P2T$
 $A(2,4) = RH02 * F1PP2T$
 $A(3,1) = RH01 * RH03 * F131P$
 $A(3,2) = RH01 * F1P2T$
 $A(3,3) = RH01 * RH03 * F1P31P - A1P$
 $A(3,4) = RH01 * RH03 * F1PP1P$
 $A(4,1) = RH01 * RH03 * F1PP31$
 $A(4,2) = RH01 * F1PP2T$
 $A(4,3) = RH01 * RH03 * F1PP1P$
 $A(4,4) = RH01 * RH03 * F1DP - A1PP$
 $B(1) = -RH01 * G1$
 $B(2) = -RH02 * W4 * P$
 $B(3) = -RH01 * G1P$
 $B(4) = -RH01 * G1PP$
 $IF(A1P.EQ.0.0) MA=2$
 $CALL LNEONS (A,MA,2)$
C B BECOMES THE SOLAR RADIOSITY
C REFLECTANCE=ENERGY OUT / ENERGY IN
16 ENRGIN=P*COS(ZPA)
 IF(MA.EQ.2) B(4)=0.
 ENGOUT=RH03**5*R+B(1)*F14T+B(2)*F24T+B(3)*F1P4T+B(4)*F1PP4T
 REFLEC=ENGOUT/ENRGIN
 CONTINUE
C CALCULATION OF Q ABSORBED AT EACH SURFACE DUE TO SOLAR RADIATION
 IF(PHI.GT.0.) GO TO 51
C FOR PHI LESS THAN OR EQUAL TO ZERO
 F23T=(2.-AE)/2.
 F1PP3T=(AC+CJ-(AC+DJ))/2.
 F1P3T=(AC+DJ-(CJ+AB))/2.
 F13T=(1.+AP-BJ)/2.
 IF(THETA.NE.90.) GO TO 92
 F1PP3T=0.
 F13T=(1.+Y1P-SQRT(1.+Y1P**2))/2.
 F1P3T=(1.+SQRT(1.+Y1P**2)-Y1P-SQRT(2.))/2.
98 CONTINUE
 QABS1=(ALPHA1/RH01)*(A1*R(1)+A1P*R(2)+A1PP*R(4))
 QABS2=(ALPHA2/RH02)*(A2*R(2))
 QABS3=ALPHA3*(P**2+F13T*R(1)+F1P2T*R(3)+F1PP2T*R(4)+F23T*R(2))
 GO TO 52
C FOR PHI GREATER THAN ZERO
 QABS1=(ALPHA1/RH01)*B(1)
 QABS2=(ALPHA2/RH02)*(A2*B(2)+A2P*(B(3)))
 F13T=(2.-ZEP)/2.
 F23T=(1.+A2-ZEP)/2.
 F2P3T=(1.+ZEP-(A2+7UP))/2.
 QABS3=ALPHA3*(P**2+F13T*B(1)+F23T*B(2)+F2P3T*B(3))
52 CONTINUE
C CALCULATION OF RADIOSITIES DUE TO TEMPERATURE

```

C      FOP TERRESTRIAL
ALPAT1=EMM1
ALPAT2=EMM2
ALPAT3=EMM3
RHOT1=1.-ALPAT1
RHOT2=1.-ALPAT2
RHOT3=1.-ALPAT3
F11T=RHOT3*(1.-SIN(ZT))
F31T=(2.-2.*SIN(ZB))/2.
F32T=(2.-2.*SIN(ZA))/2.
OS=SIN(ZB)+SIN(ZA)-1.
IF(THETA.GE.60.)F12T=OS+(RHOT3/2.)*(1.+HG-(AE+HJ))
IF(THETA.LT.60.)F12T=OS+(RHOT3/2.)*(2.-AE)
QS3=EMM3*SIGMA*(T3**4)
C      AREAS OF BLADES AND BASE
A1=1.
A2=1.
A3=1.
A(1,1)=RHOT1*F11T-A1
A(1,2)=RHOT1*F12T
A(1,3)=A1*EMM1*SIGMA
B(1)=-RHOT1*QS3*F31T
A(2,1)=RHOT2*F12T
A(2,2)=-A2
A(2,3)=A2*EMM2*SIGMA
B(2)=-RHOT2*QS3*F32T
A(3,1)=ALPAT1*F11T+ALPAT2*F12T
A(3,2)=ALPAT1*F12T
A(3,3)=-A1*SIGMA*(EMM1+EMM2)
B(3)=-(QABS1+QABS2+ALPAT1*QS3*F31T+ALPAT2*QS3*F32T)
MA=3
CALLLNEQNS(A,MA,B)
RAD1=B(1)
RAD2=B(2)
T1=SQRT(SQRT(B(3)))
RQABS1=RAD1*ALPAT1/RHOT1
RQABS2=RAD2*ALPAT2/RHOT2
RQABS3=ALPAT3*(RAD1*F31T+RAD2*F32T)
E1=EMM1*SIGMA*(T1**4)
E2=EMM2*SIGMA*(T1**4)
G1=ALPAT1*(RAD1-E1)/RHOT1
G2=ALPAT2*(RAD2-E2)/RHOT2
QNET3=QS3-(QABS3+RQABS3)
WRITE(6,60)THETA,PHI,QABS1,QABS2,QABS3,RQFLEC,G1,G2,RQABS3,RAD1,
1 RAD2,T1,QNET3
60  FORMAT(1X,2F6.1,11F6.2)
10  CONTINUE
STOP
END

```

SENTRY

	5.0	5.0	
.8	.8	.9	442.
0.	90.	-90.	90.
.2	.2	.1	
.1	.1	.05	530.

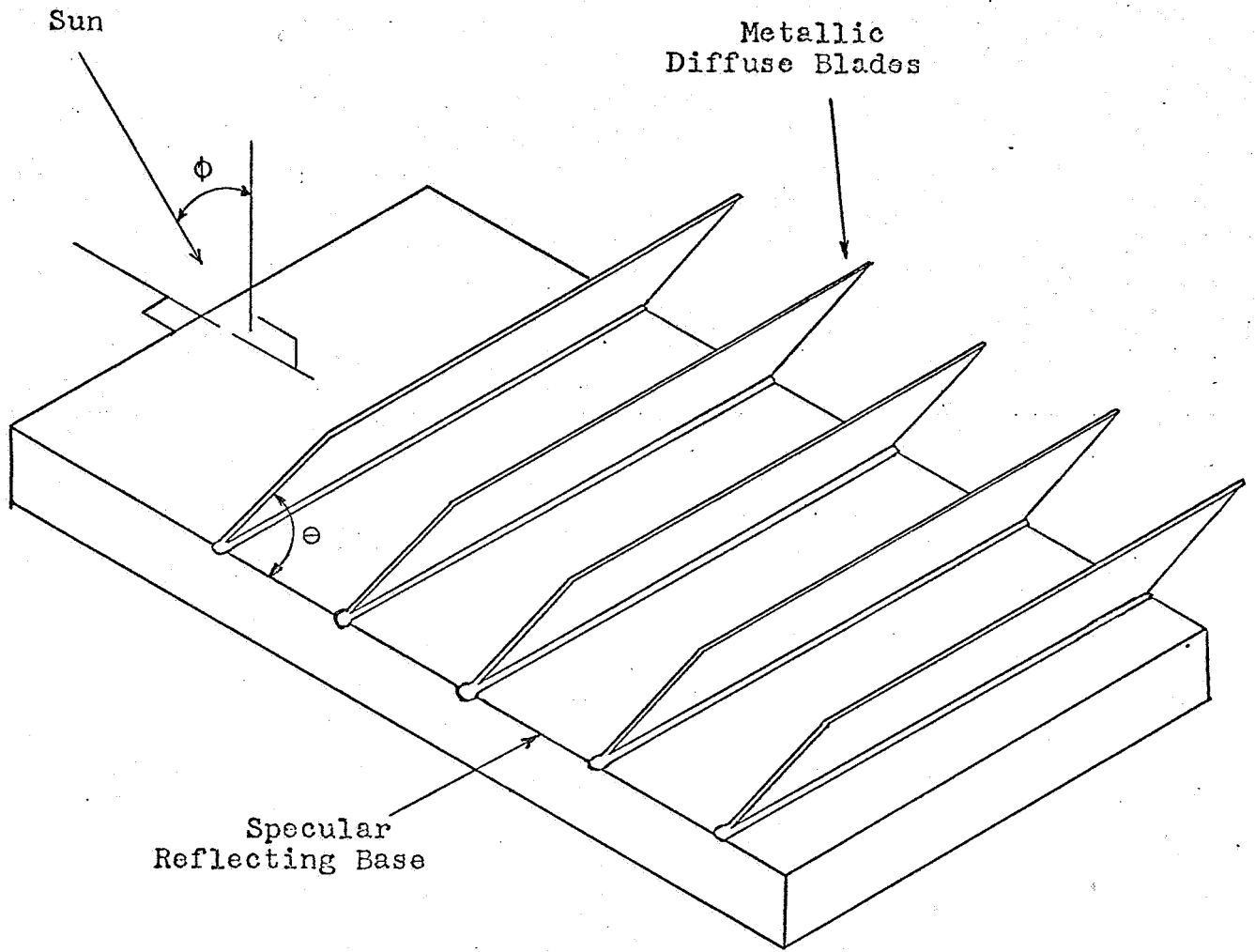
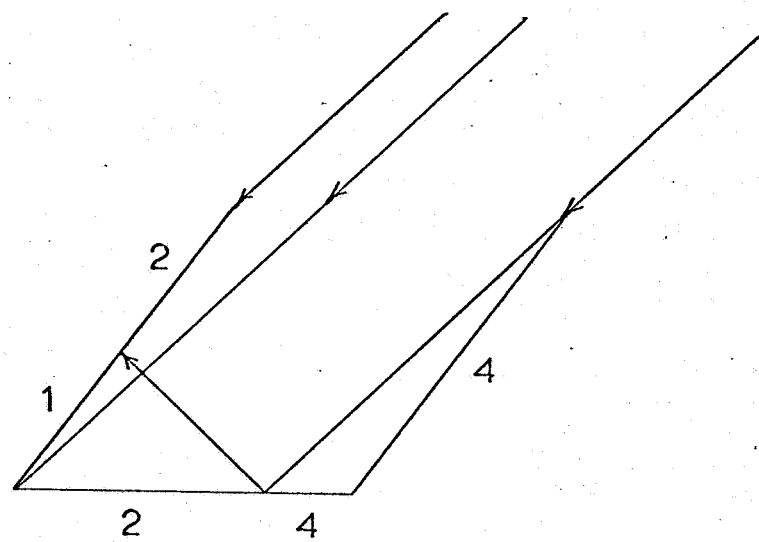


FIGURE 1 NEW TYPE LOUVER CONFIGURATION

SUN.



SUN

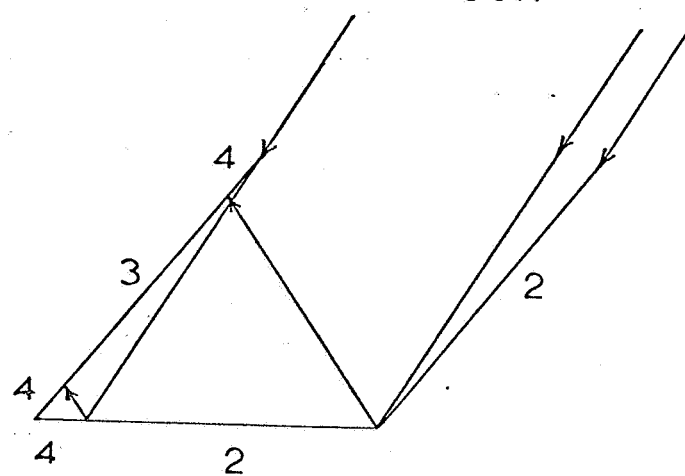


FIGURE 2 METHODS OF ILLUMINATION

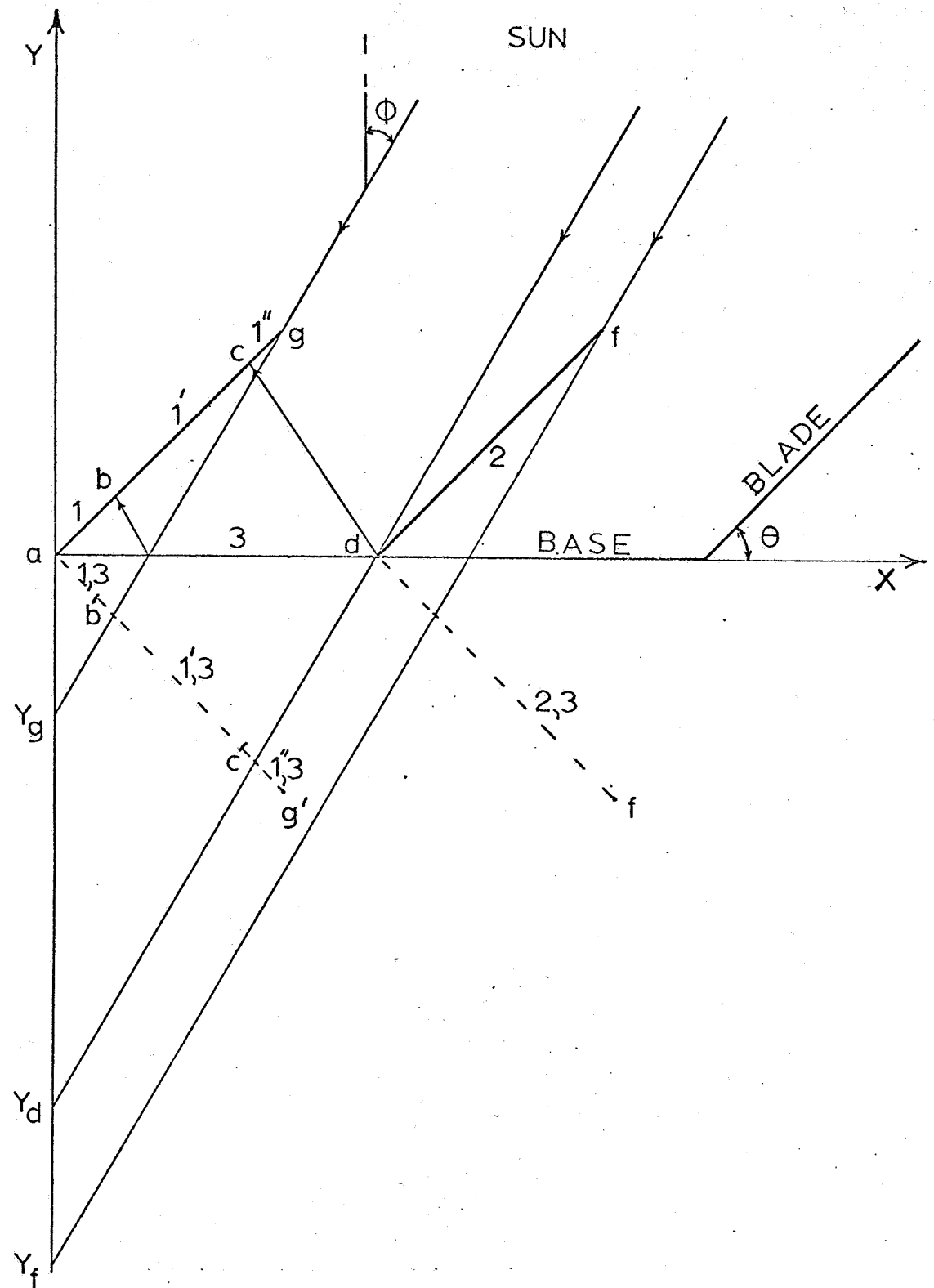


FIGURE 3 SCHEMATIC DIAGRAM FOR ILLUMINATION OF LOUVERS

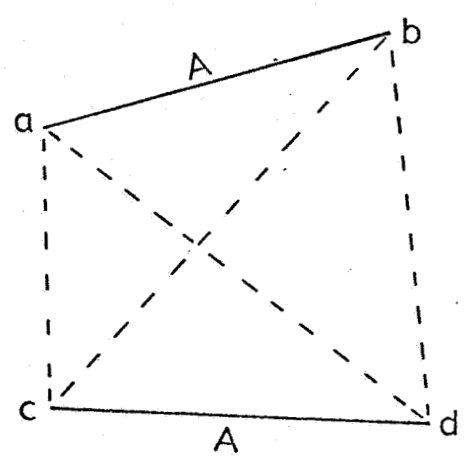


FIGURE 4 HOTTEL'S CROSSED STRING METHOD

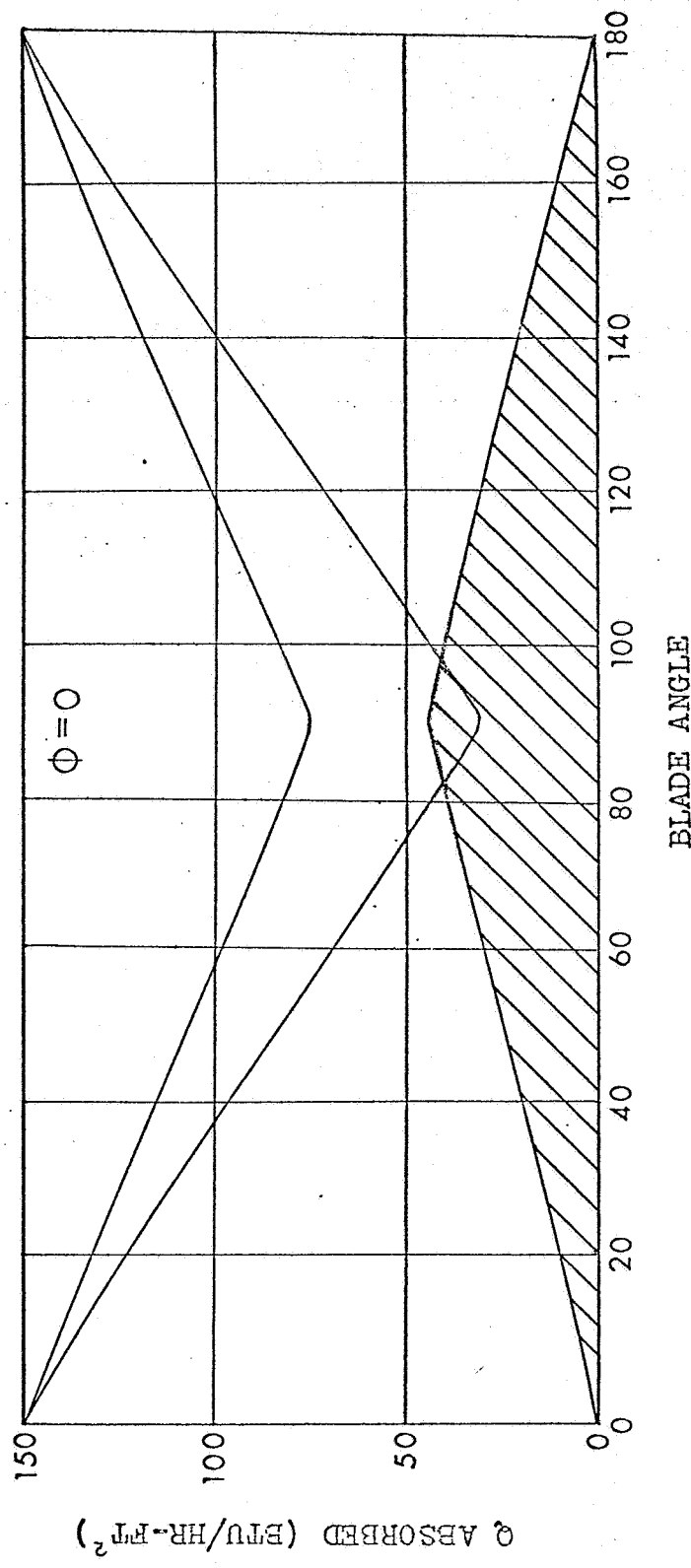
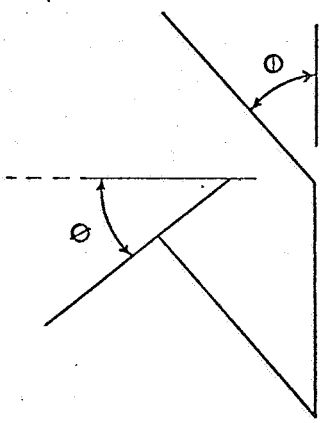
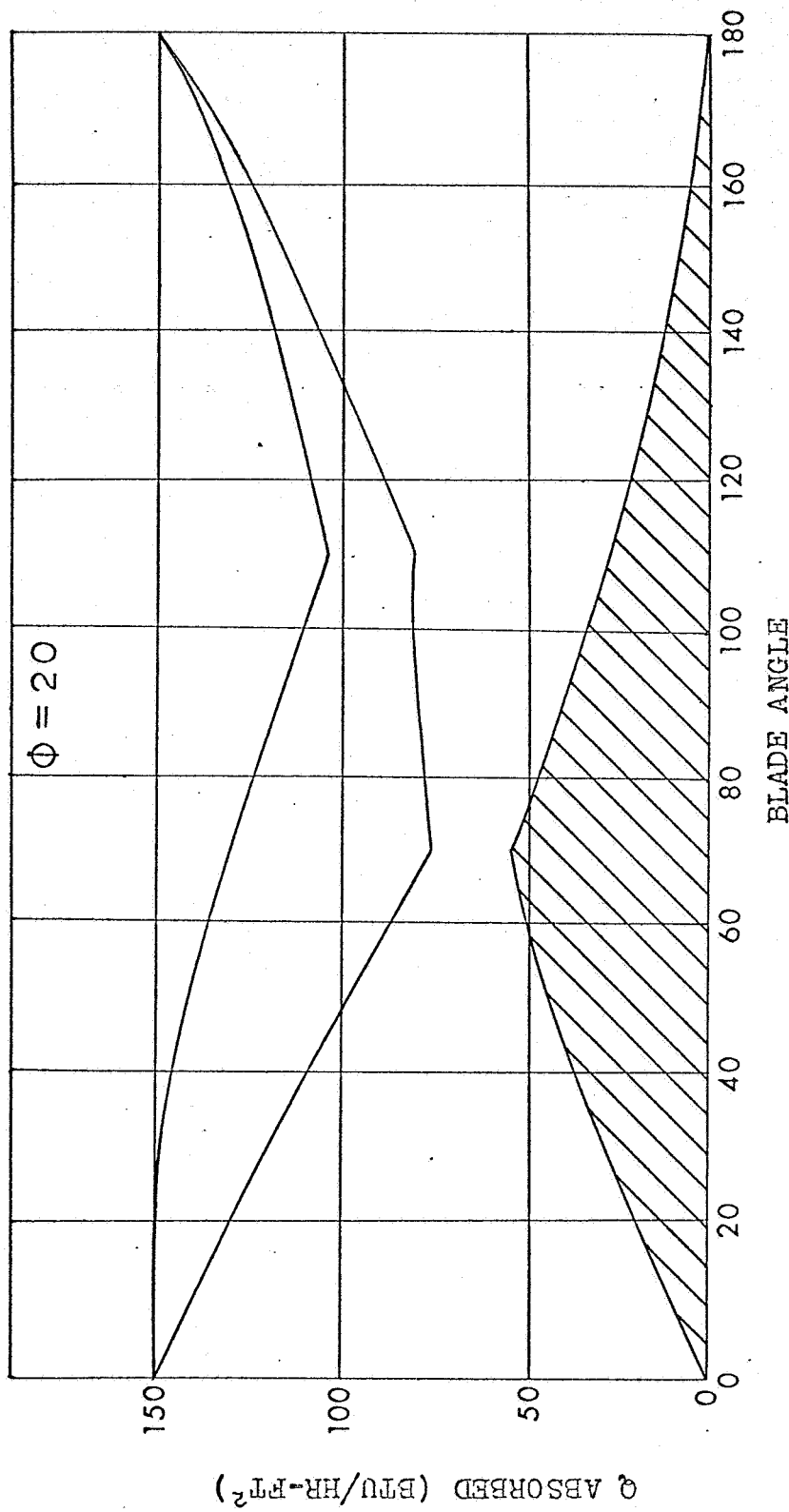


FIGURE 5a COMPONENTS OF Q ABSORBED BY BASE SURFACE

FIGURE 5b COMPONENTS OF Q ABSORBED BY BASE SURFACE



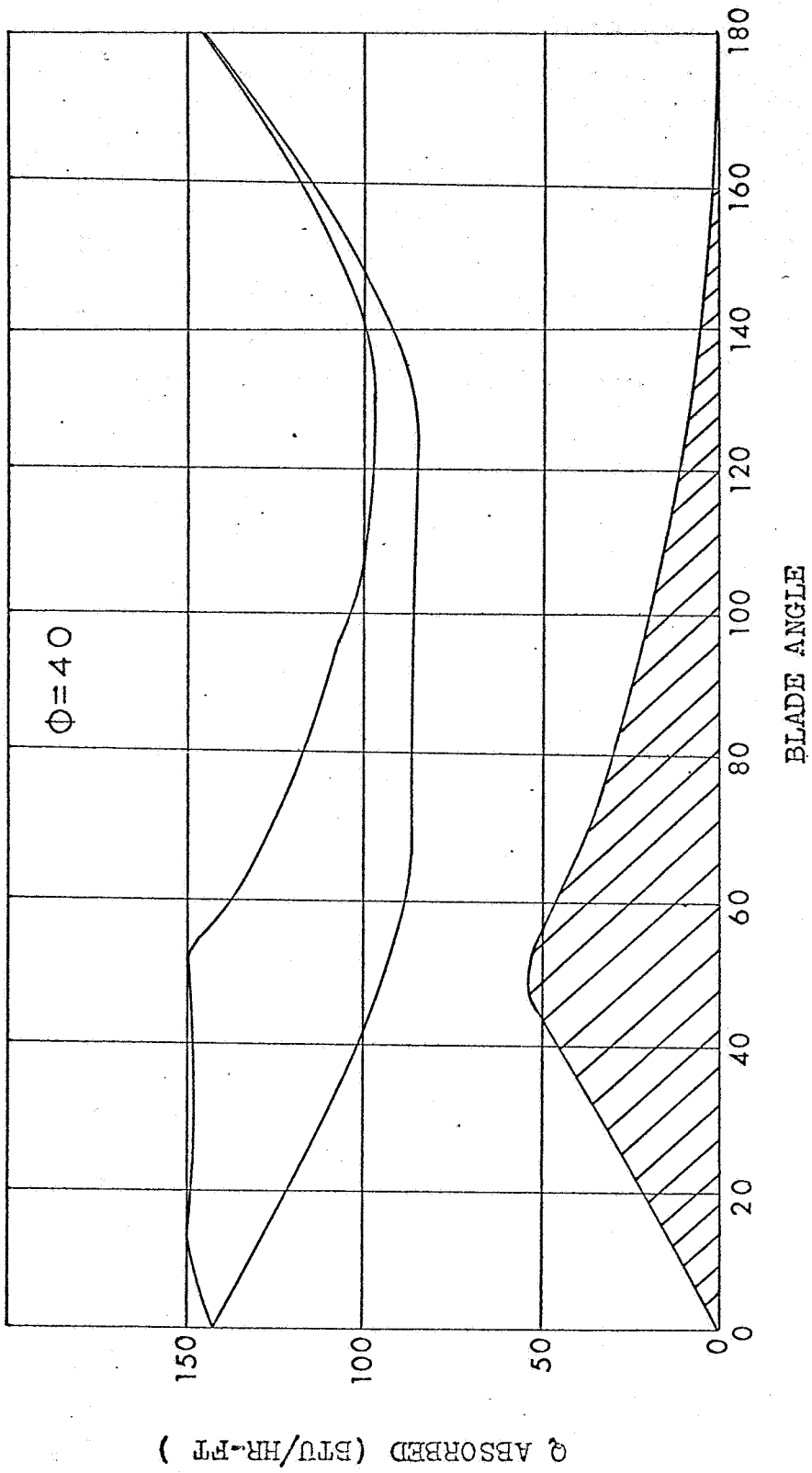


FIGURE 5c COMPONENTS OF Q ABSORBED BY BASE SURFACE

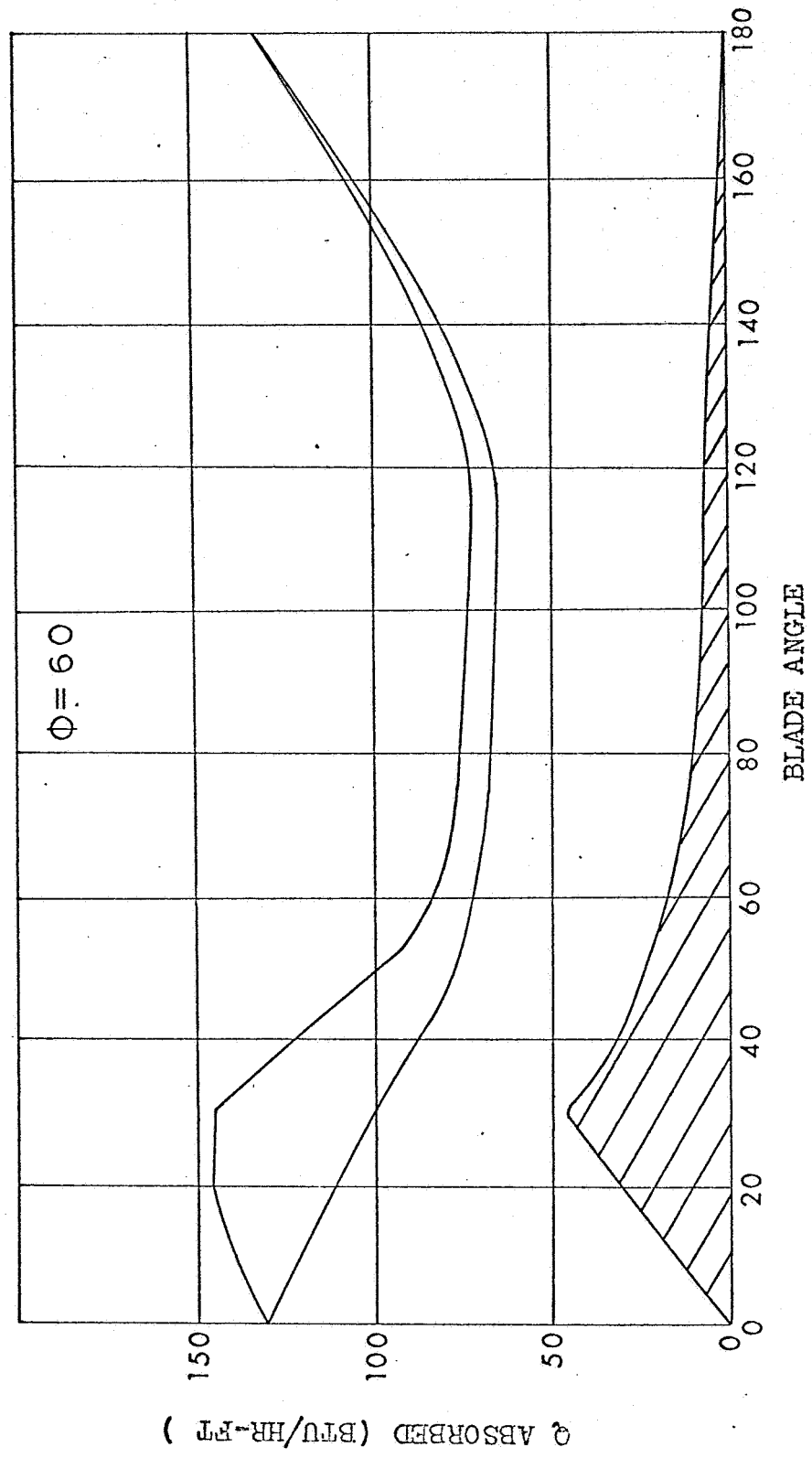


FIGURE 5d COMPONENTS OF Q ABSORBED BY BASE SURFACE

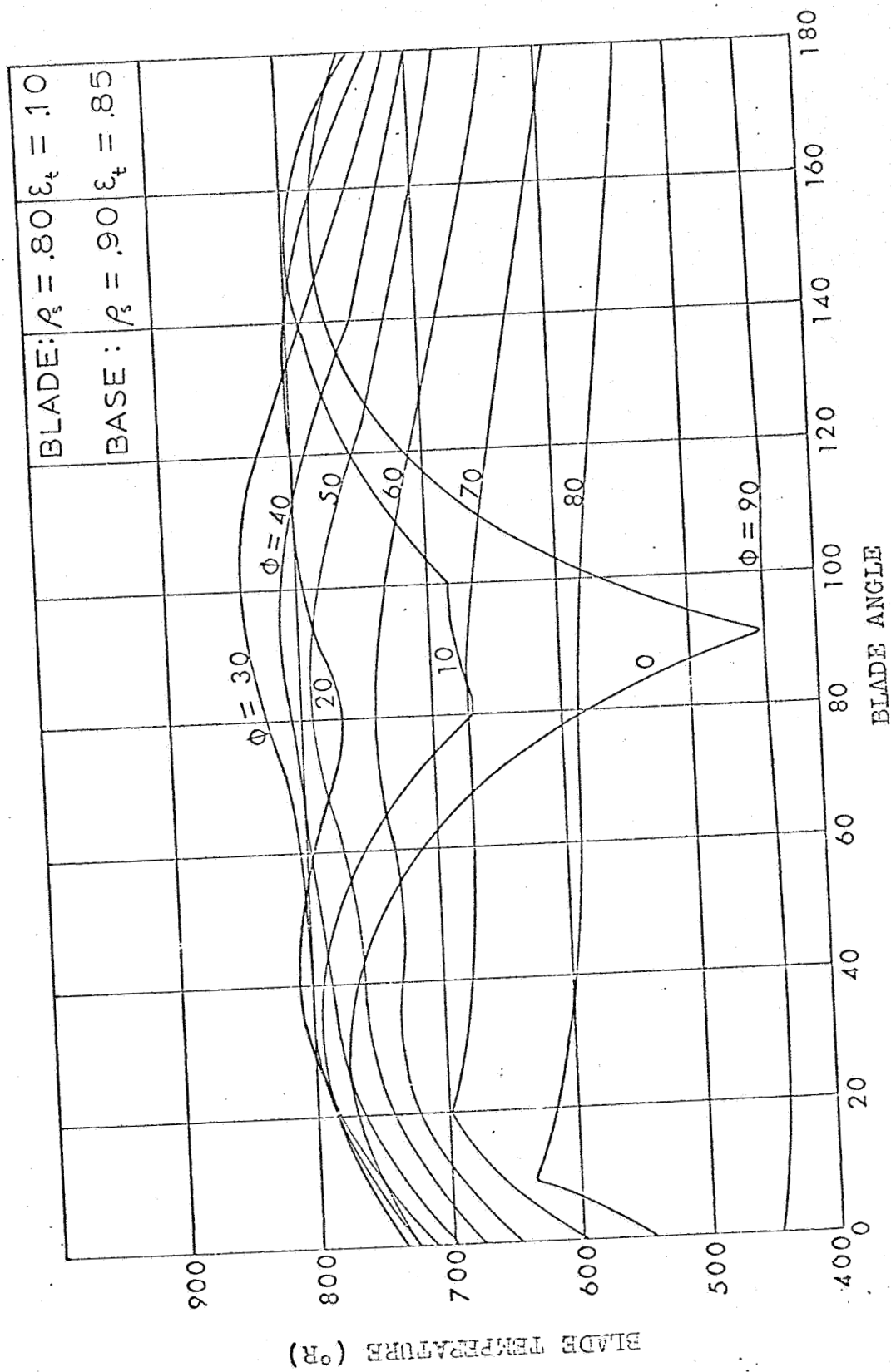


FIGURE 6.8 TEMPERATURE OF LOUVER BLADES

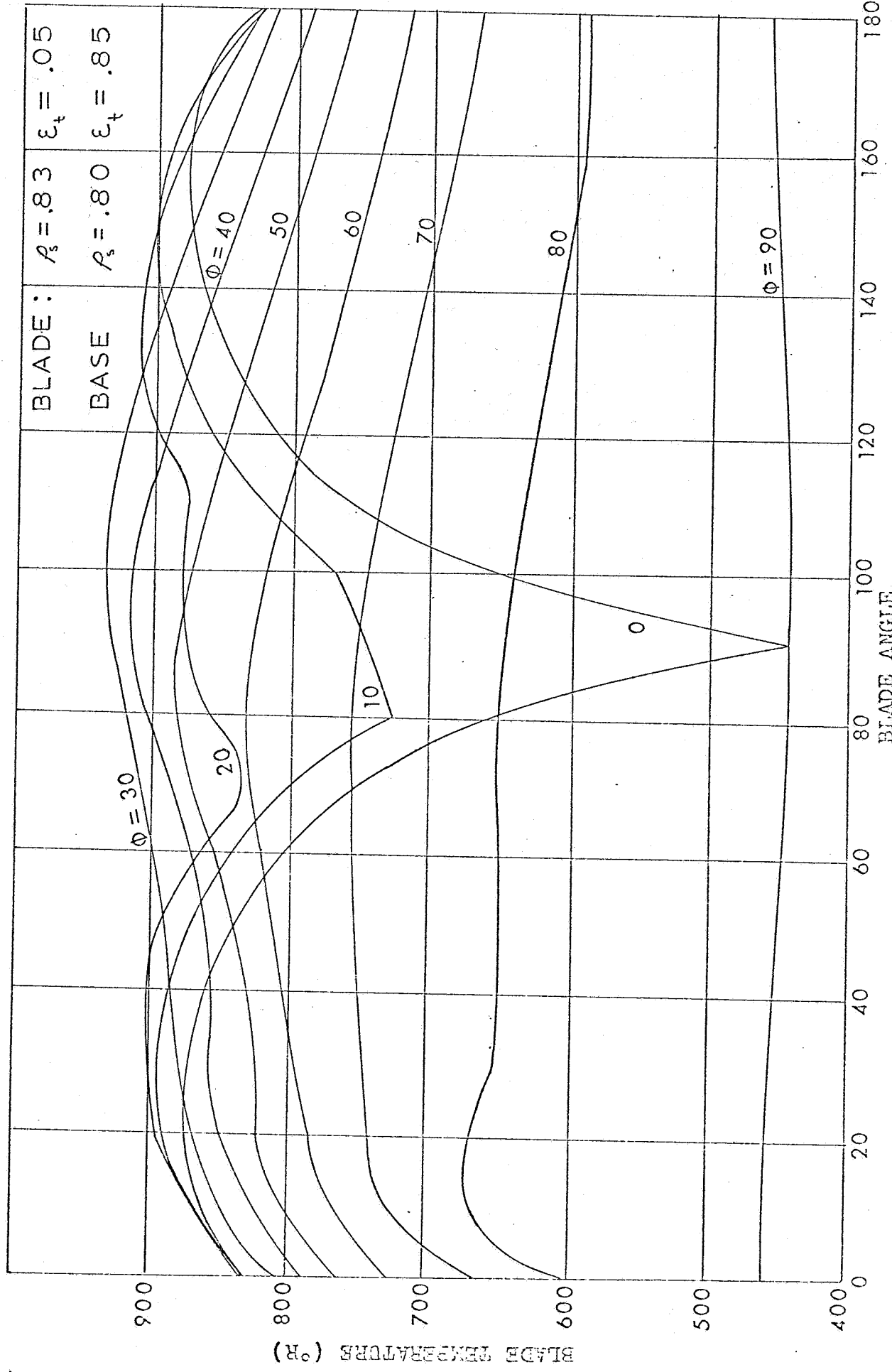


FIGURE 16, TEMPERATURE OF LOUVER BLADES

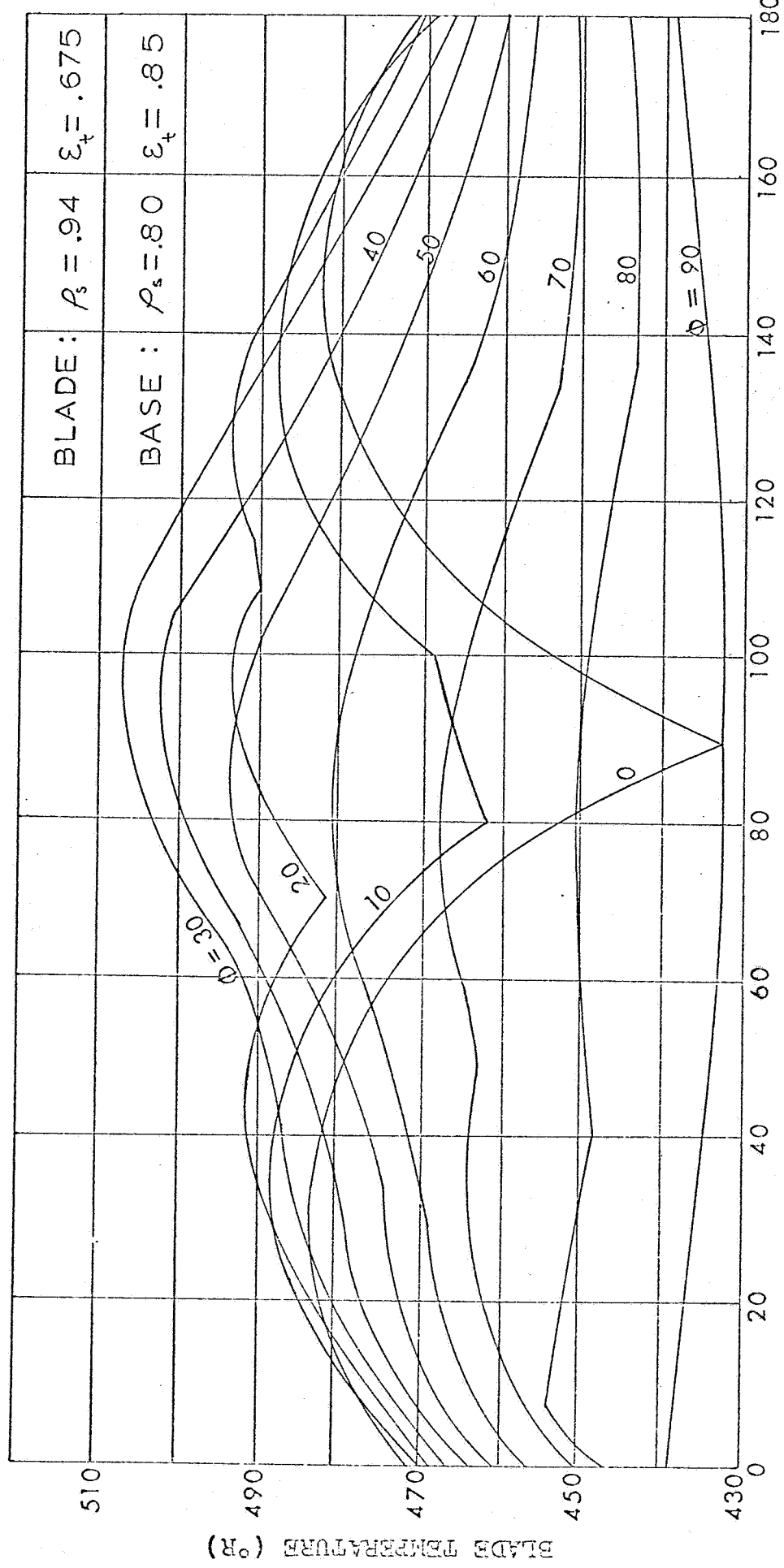


FIGURE 16c TEMPERATURE OF LOUVER BLADES

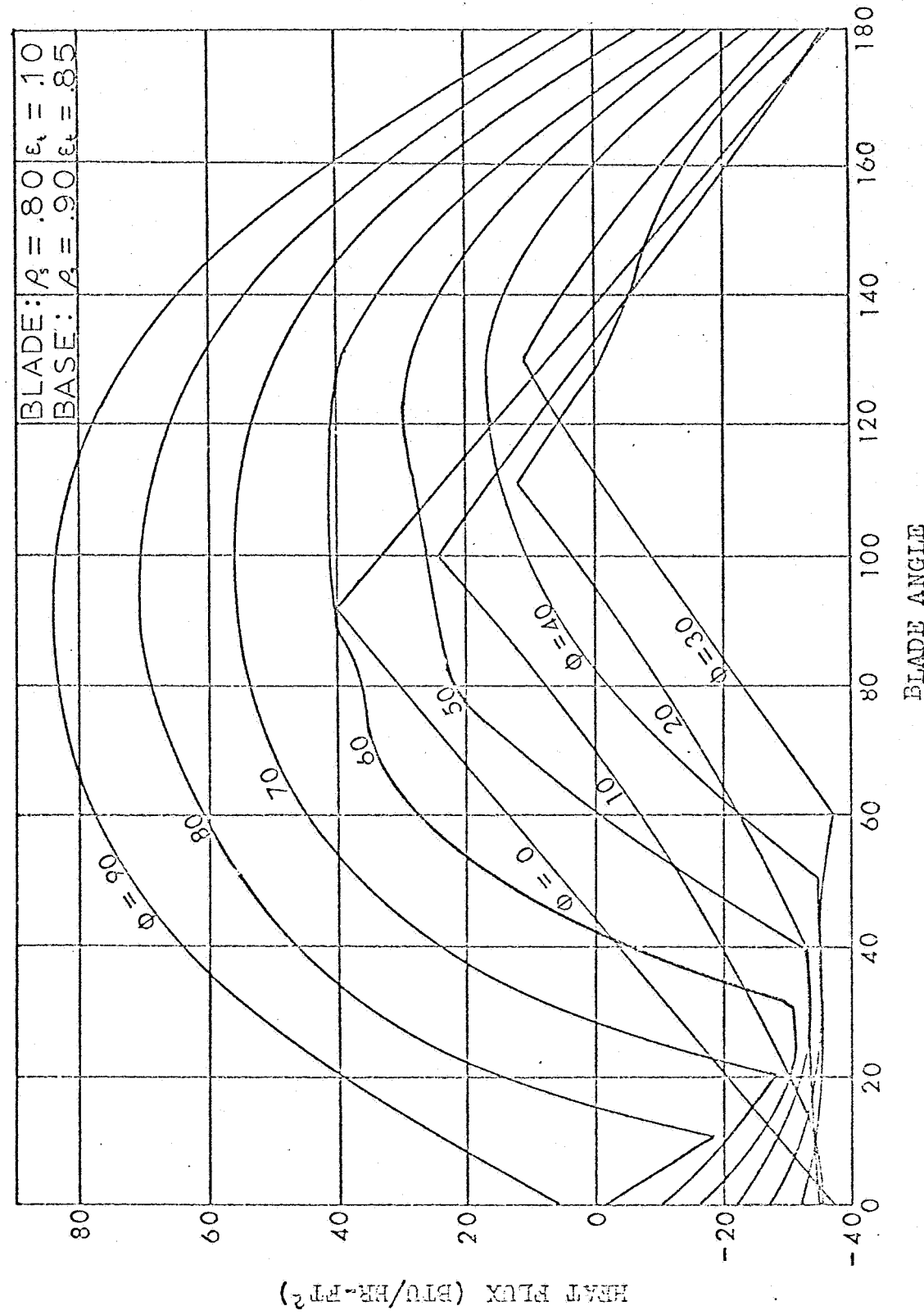


FIGURE 7 & HEAT REJECTION CAPABILITY OF BASE SURFACE

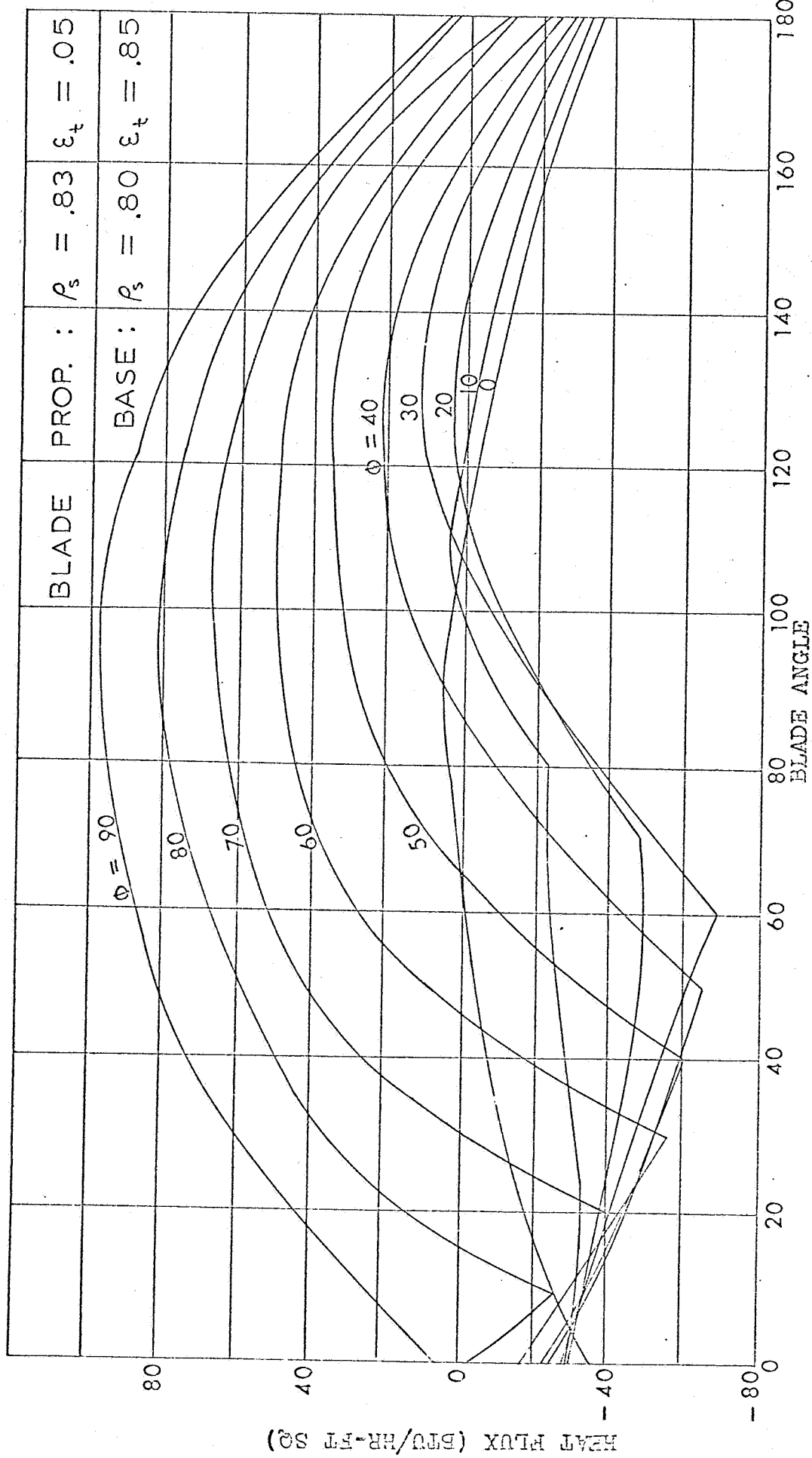


FIGURE 7b HEAT REJECTION CAPABILITY OF BASE SURFACE

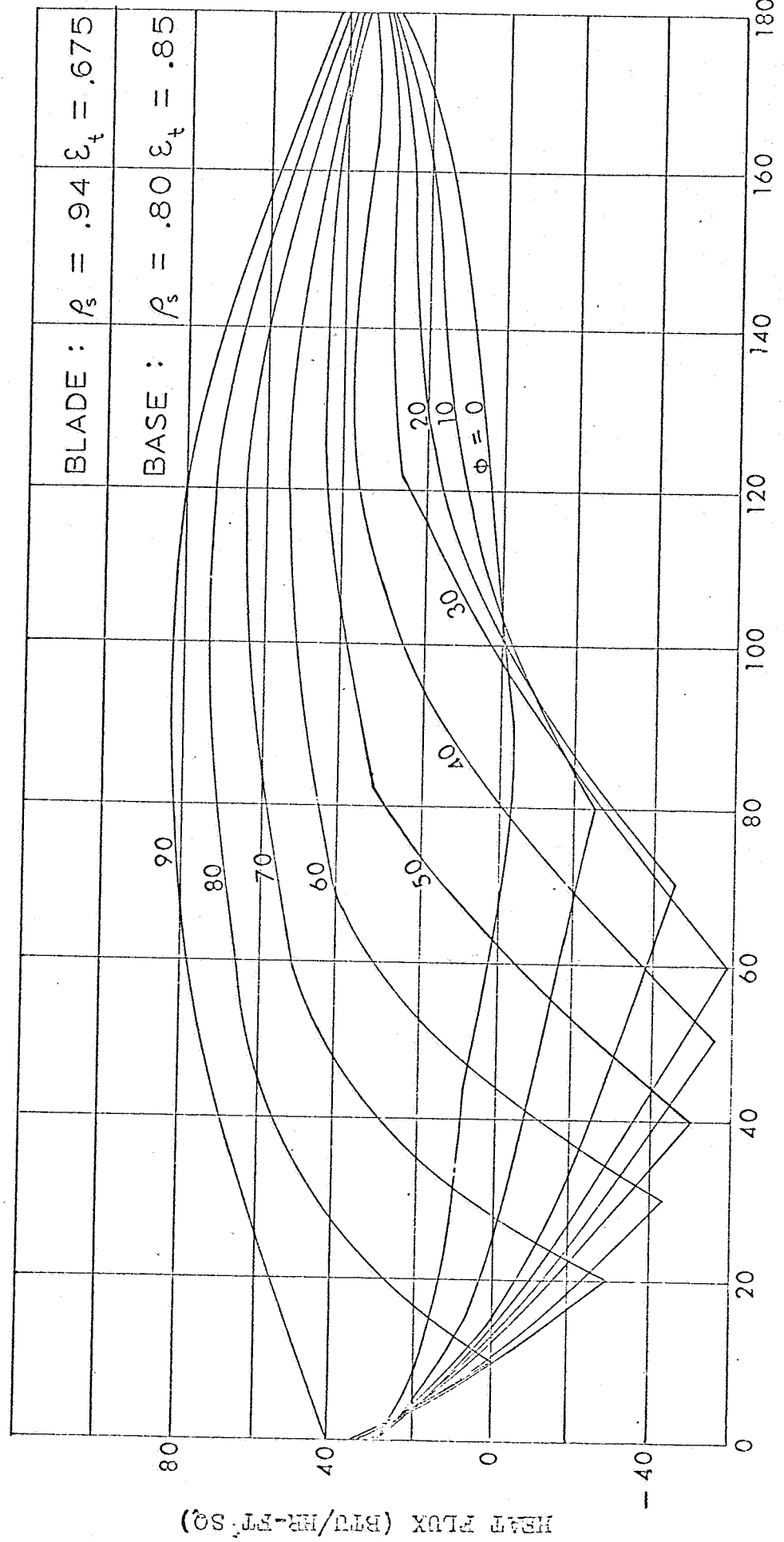


FIGURE 7c HEAT REJECTION CAPABILITY OF BASE SURFACE

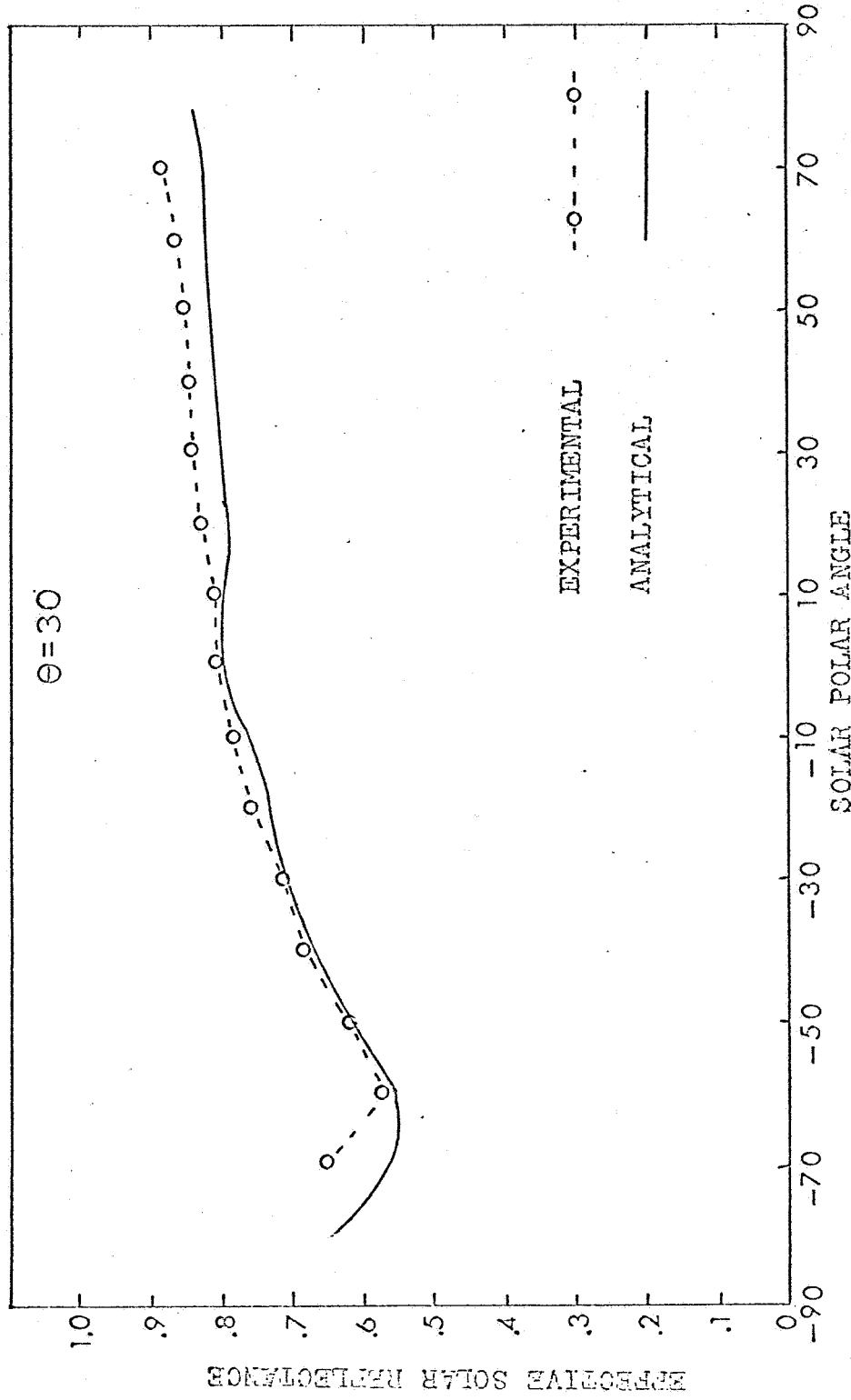


FIGURE 8-a EFFECTIVE SOLAR REFLECTANCE OF LOUVER TEST MODEL

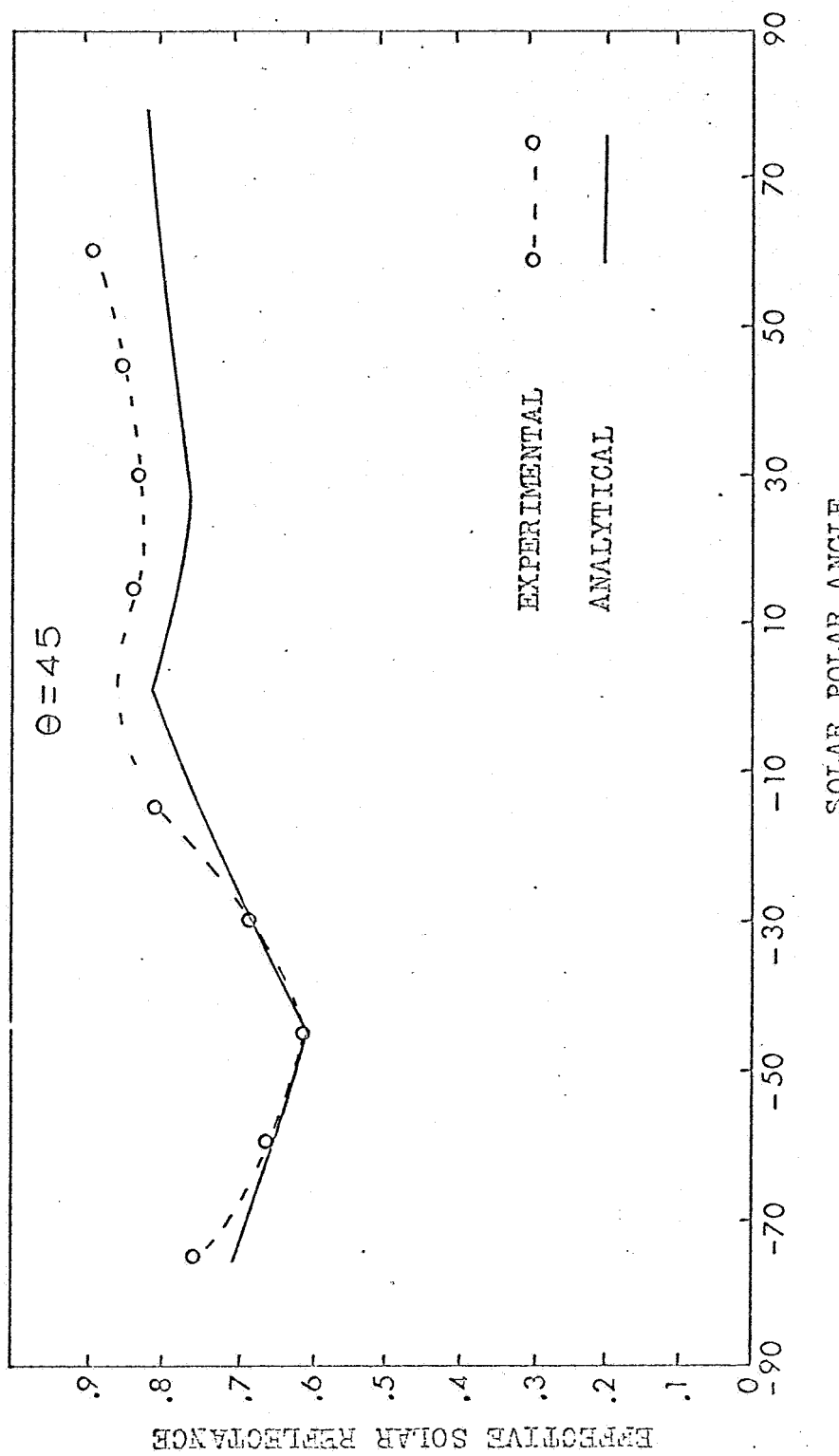


FIGURE 8b EFFECTIVE SOLAR REFLECTANCE OF LOUVER TEST MODEL

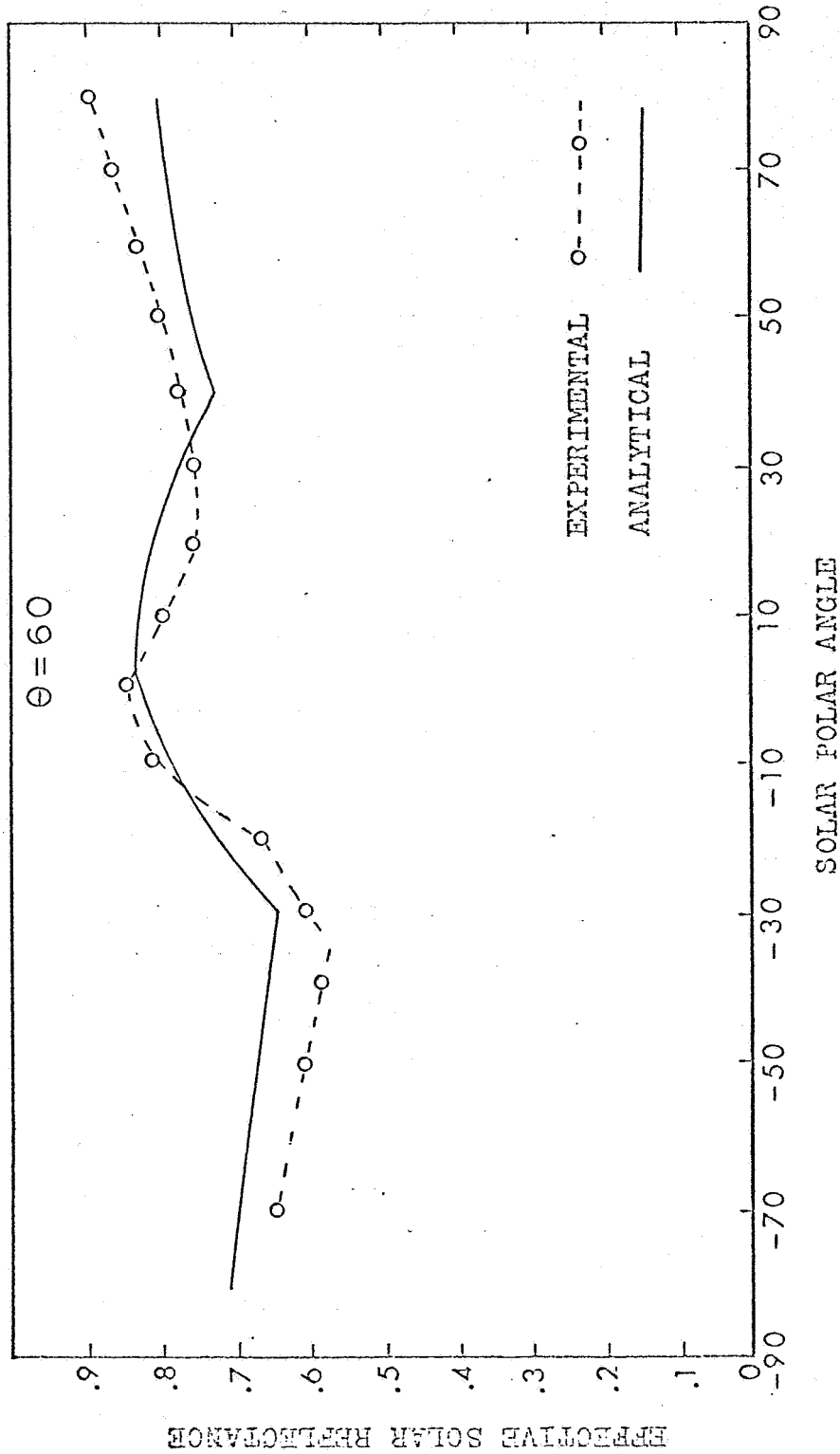


FIGURE 8c EFFECTIVE SOLAR REFLECTANCE OF LOUVER TEST MODEL

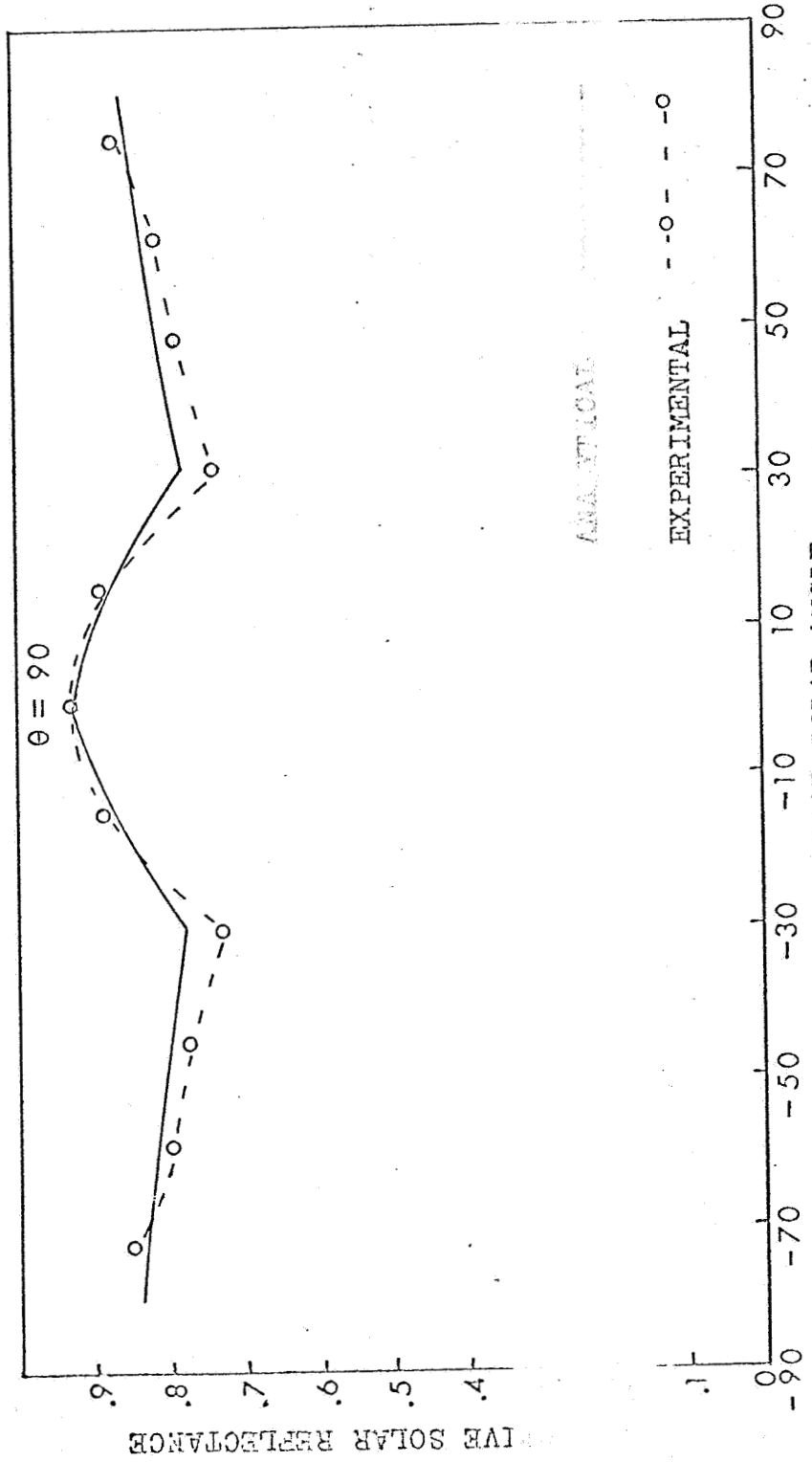


FIGURE 8d EFFECTIVE SOLAR REFLECTANCE OF LOUVER TEST MODEL